UNIVERSITY OF THE STATE OF BAHIA

DEPARTMENT OF EXACT AND EARTH SCIENCES

POSTGRADUATE PROGRAM IN BIOSYSTEMS MODELING AND SIMULATION

LAÍS DAS NEVES SANTANA

ECONOMIC MODELING OF THE DESTRUCTIVE POTENTIAL RESULTING FROM EXTREME RAIN EVENTS

ALAGOINHAS – BA

2023

LAÍS DAS NEVES SANTANA

ECONOMIC MODELING OF THE DESTRUCTIVE POTENTIAL RESULTING FROM EXTREME RAIN EVENTS

Dissertation presented to the Postgraduate Course in Modeling and Simulation of Biosystems at the State University of Bahia in fulfillment of the requirement for the defense of the dissertation.

Advisor: Prof. Dr. Alarcon Matos de Oliveira

ALAGOINHAS – BA

2023

CATALOGRAPHIC SHEET

Library Systems UNEB
Library Carlos Drummond de Andrade – *Campus II*
Manoela Ribeiro Vieira
Librarian - CRB 5/1768

S232m Santana, Laís das Neves

Economic modeling of the destructive potential resulting from extreme rainfall events / Laís das Neves Santana – Alagoinhas, 2023

69 f.: il

Advisor: Prof. Dr. Alarcon Matos de Oliveira.

Dissertation (Mestrado) – University of the State of Bahia, Derpartment of Exact and Earth Scienses. Postgraduate Program in Biosytems Modeling and Simulation. Mestrado in Biosytems Modeling and Simulation – Alagoinhas,2023.

1. Floods – Catu BA 2. Economic modeling 3. Geoprocessing I. Oliveira, Alarcon Matos de. II. University of the State of Bahia – , Derpartment of Exact and Earth Scienses – Campus II. III. Título

CDD – 627.42

SHEET IN APPROVAL

"MODELING ECONOMIC OF POTENTIAL DESTRUCTIVE IN RESULT OF EXTREME RAIN EVENTS."

LAÍS DAS NEVES SANTANA

Dissertation presented to the Postgraduate Program in Biosystems Modeling and Simulation – PPGMSB, on October 23, 2023, as a partial requirement to obtain the Master's degree in Biosystems Modeling and Simulation from the State University of Bahia, as assessed by the Board Examiner:

gov.br Documento assinado digitalmente
ALARCON MATOS DE OLIVEIRA
Data: 23/10/2023 17:03:02-0300
Verifique em https://validar.iti.gov.br

Teacher Dr. ALARCON MATOS IN
OLIVEIRA UNEB
Doctorate degree in Geography (Geography
Physics) University of São Paulo

gov.br Documento assinado digitalmente
MARIA DOLORES RIBEIRO ORGE
Data: 23/10/2023 17:11:04-0300
Verifique em https://validar.iti.gov.br

Teacher Dr. MARIA DOLORES RIBEIRO
ORGE UNEB
Doctorate degree in Ecology y Average
Environment Complutense University of
Madrid

gov.br Documento assinado digitalmente
ROSANGELA LEAL SANTOS
Data: 23/10/2023 17:15:16-0300
Verifique em https://validar.iti.gov.br

Teacher Dr. ROSÂNGELA LOYAL
SANTOS UEFS
Doctorate degree in Engineering in
Transport University of São Paulo

DEDICATION

Firstly, to God, all honor and glory, to my parents, Marinalva das Neves Santana and Josevaldo dos Santos Santana (*in memoriam*), to my brothers and my family as a whole and to my beloved friends.

THANKS

To God for allowing me to pass the selection process and allowing me to combine my work and my master's degree and for supporting me throughout the course and especially in the last few months, guiding me so that I had the opportunity to qualify.

I thank my parents for always encouraging me in my studies and my sisters and brother for teaching me to read and write and helping me to enter university.

To my friends, especially master's student Carlina Aparecida, who has been with me since graduation, Telma Costa and Cintia Porto, also a master's student in the program, and my other friends for supporting me and rooting for me to reach this new stage.

To the advisor Professor Alarcon Matos de Oliveira, for all the partnership, patience, understanding and professionalism throughout this time, I left the choice of my advisor in the hands of the Lord and He chose him, so I can only thank you for everything.

To Racquel and Catugy for helping me in the critical phase of my research, where Racquel introduced me to my unofficial co-supervisor.

Fabricio Garcia, despite not being able to have his name in the research as he was still completing his doctorate, helped me with the modeling part, thus enabling me to obtain the necessary data for qualification.

To Professor José Roberto, known as Zé, for all the support and guidance since graduation and for sending me the program registration notice and for welcoming me during the internship.

To the State University of Bahia for all the opportunities given to me.

To my co-workers for all their encouragement in achieving this new stage in my life.

To Professor Marcos, for helping me when it was difficult to change topics.

To Professor Thayse Fonseca, for her support in the final stretch of the dissertation.

To the PPGMSB program, for helping students in the process throughout the master's degree.

Anyway, to everyone who, in some way, helped me to be where I am today, THANK YOU SO MUCH.

Reveal your tasks to the Lord, and your projects will come true. Pr, 16, 3.

RESUMO

As inundações são um problema recorrente em muitas cidades do Brasil, resultando em prejuízos significativos tanto pessoais quanto para a economia da cidade, tais como, na saúde, materiais, financeiros e para o meio ambiente como um todo. O município de Catu, no estado da Bahia, também vem sofrendo com esse cenário, com pontos críticos de inundação no bairro da Santa Rita nas redondezas do centro de abastecimento, no centro da cidade e em alguns bairros. Esta pesquisa concentrou-se em analisar o potencial destrutivo de chuvas intensas na região da Santa Rita (Centro de Abastecimento) de Catu - BA, utilizando softwares de simulação baseados em tecnologias computacionais e de geoprocessamento, como HEC RAS, HEC HMS e o QGis 3.16, utilizando a modelagem bidimensional. Os resultados revelaram que a área em questão se torna praticamente intransitável durante eventos de inundação, causando perdas econômicas significativas, principalmente para os feirantes locais.

Palavras-chave: Inundações. Modelagem. Geoprocessamento.

ABSTRACT

Floods are a recurring problem in many cities in Brazil, resulting in significant losses both personally and to the city's economy, such as health, material, financial and the environment as a whole. The municipality of Catu, in the state of Bahia, has also been suffering from this scenario, with critical flooding points in the Santa Rita neighborhood, close to the supply center, in the city center and in some neighborhoods. This research focused on analyzing the destructive potential of intense rains in the Santa Rita region (Supply Center) of Catu - BA, using simulation software based on computational and geoprocessing technologies, such as HEC RAS, HEC HMS and QGis 3.16, using two - dimensional modeling. The results revealed that the area in question becomes practically impassable during flood events, causing significant economic losses, especially for local stallholders.

Keywords: Floods. Modeling. Geoprocessing.

LIST OF FIGURES

LIST OF FRAMES

LIST OF TABLES

LIST OF EQUATIONS

LIST OF ACRONYMS

ANA	National Water Agency
CN	Curve Number
CN-SCS	Curve Number – Soil Conservation Service
EMBRAPA	Brazilian Agricultural Research Company
GRG	Generalized Reduced Gradation
HEC	Hydrologic Engineering Center
IBGE	Brazilian Institute of Statistics
IDEB	Basic Education Development Index
ID	Economic Indicators
HDI	Human Development Index
IDF	Intensity Duration Frequency
INCT	National Institute of Science and Technology
LPI	Local Partial Inertia
MDT	Digital Terrain Model
SRTM	Topographic Radar Shuttle Mission
PEA	Economically Active Population
GDP	Gross Domestic Product
PVA	Red-Yellow Ultisols
SEI	Superintendency of Economic and Social Studies of Bahia
UNET	Unsteady NETwork Model
USACE	Army Corps of Engineers

SUMMARY

1 INTRODUCTION

The flood scenario is recurrent in several cities in Brazil, resulting in various losses, both personal and economic, such as health, material goods, finances and environmental impacts. The municipality of Catu is no exception, facing flooding in several areas, including the Santa Rita neighborhood, in the vicinity of the Supply Center, in the city center, and other streets in the city.

Furthermore, floods caused by intense rains pose risks, such as dragging people, damaging vehicles and the possibility of illnesses resulting from contamination by sewage water, negatively impacting local businesses. At certain times of the year, high rainfall can result in disasters, including flooding of homes, commercial establishments and religious temples.

According to Freitas and Ximenes (2012), these floods tend to occur in more vulnerable areas, such as poorer and more peripheral regions that are generally occupied in a disorderly manner and on slopes susceptible to landslides. Because of these issues, the region of the Santa Rita neighborhood was chosen for the study, where the Catu Supply Center is located, where the street market and several other commercial points operate on the banks of the Catu river and the existing dam in the city. .

Given the complex and disorderly urban occupation, this study aimed to analyze the economic implications arising from extreme rainfall events, experienced by residents and traders (marketers and shopkeepers) of the Catu Supply Center, to identify possible solutions that public managers can adopt. Given the above, the question that guided this study was: What are the economic impacts of extreme rainfall in Catu-Bahia (Brazil)?

1.1 Goals

1.1.1 Main goal

Analyze the destructive potential of intense rains in the Santa Rita region, where the Catu Supply Center (Bahia) is located, through the use of simulation software.

1.1.2 Specific objectives

- Assess the economic losses caused by flooding at different return times, in order to understand its impact on the community;
- Carry out simulations to model and analyze hydrological and hydrodynamic behavior in intense precipitation events, in order to identify areas of greatest vulnerability and understand flooding patterns.

1.2 Hypothesis

The hypothesis of this study is that, through the analysis of the economic impact resulting from floods caused by intense rain, it will be possible to identify and propose solutions that minimize damage to the local community. It is believed that by understanding the costs and economic damages associated with floods, it will be possible to develop strategies and adaptation measures that contribute to a more resilient and sustainable coexistence with heavy rain events.

2 THEORETICAL REFERENCE

2.1 Hydrological Risks

Hydrology encompasses the study of natural phenomena present in the hydrological cycle, such as precipitation, evaporation, infiltration and runoff in rivers. However, the analysis of these characteristics is complex due to the influence of several interconnected factors (Marinho Filho, 2012).

Hydrological models are fundamental tools used to represent the processes that occur in river basins and predict the consequences in relation to observed values. The objective of a hydrological model is to efficiently determine the components of the hydrological cycle in a river basin and accurately estimate the behavior and magnitude of water flow (Marinho Filho, 2012).

hydrometeorological risks associate certain meteorological events capable of generating intense precipitation, that is, a large amount of rain concentrated in a short period of time and in a certain geographic region.

Monte *et al.* (2021) highlight that human civilization faces several natural dangers with the potential to produce disasters, the classification of which is related to the triggering of events. The authors emphasize that activities carried out in personal relationships, such as the division of labor, the economic-political system and production relations, when extended to the environment, can create disastrous conditions due to inadequate management of these sectors in relation to the environment.

River or oceanic hydrological episodes, capable of transporting enormous volumes of water across the Earth's surface through voluminous flows, often result in floods, which are among the deadliest natural catastrophes that have hit humanity. These catastrophes may be associated with tides that reach coastal areas, causing a high number of fatalities and displacement (Lourenço; Nunes, 2018).

According to Okada (2019), studies of the hydrological cycle, concomitant with climate change, are fundamental, especially when addressing precipitation projections, which are still uncertain. The author emphasizes that the rapid increase of humanity after the era of industrialization resulted in drastic changes in how the population began to use the soil.

It is of great relevance to deepen the studies of hydrological resources, since they play a fundamental role in the mitigation of catastrophes, as well as in studies of slope runoff.

2.2 Return time

According to Prina and Trentin (2018), the recurrence time is the inverse of the probability of an event occurring, representing the average period in which the event can occur again. This concept is crucial in the assessment and prediction of hydrological events. Taking as a starting point the risks inherent to flooding caused by large volumes of rainfall, hydrological risk emerges from a compromise between almost absolute protection and the concern to limit the costs involved in the implementation and operation of rainwater management projects (Kurek, 2012).

The risk of a flood is defined based on the vulnerability of the location. The consequences of a flood can be worsened based on the occupation of the affected area. For example, the repercussions will be different if a flooded area is a busy commercial area compared to a simple parking lot (Kurek, 2012).

According to Tucci (1993), “the choice of return time is arbitrary and depends on the definition of future zoning”. In other words, depending on the result obtained in the return time (the elevation quota corresponds to a certain return time), the future zoning (of risk) will be linked to this issue.

Therefore, understanding return time and its use in hydrological risk assessment is essential for making informed decisions about flood management and implementing disaster mitigation strategies. This approach considers the probability of future events and the vulnerability of affected areas, ensuring a balance between the safety and efficiency of investments in flood control projects.

2.3 Weather of Extreme Events (Drought and Rain)

Extreme events represent climatological occurrences that deviate from the analysis standard, covering periods of drought, high frequency of droughts, intense rains, and other superficial climatic characteristics (Rodrigues *et al.*, 2020).

Extreme weather events, whether drought or rain, cause impacts on various temporal scales. Extreme rainfall events typically occur over short periods, covering just a few days with intense rainfall. On the other hand, drought events manifest on a broader temporal scale, even extending over several years. These episodes are characterized by a prolonged drought, marked by a constant decrease in water reserves (Santos *et al.,* 2017).

According to Silva *et al.* (2020), extreme meteorological and climate events are an intrinsic part of climate variability, and their frequency and intensity can vary in response to climate change. This climate variability, through cycles, results in excesses or deficits of rainfall throughout the world, triggering droughts and floods.

These extreme events have caused significant impacts, affecting both the environment and the communities that inhabit the affected areas. These impacts include droughts, floods and landslides that occurred in urban centers, resulting in loss of life, homelessness, material damage, illnesses, environmental impacts and a series of disastrous situations (Pereira *et al.,* 2020).

Considering the city of Catu, rain occurs throughout the year. May is the rainiest month, with an average of 148 millimeters of rainfall, particularly in the autumn and winter seasons, while January is the least rainy month, characteristic of summer (Weatherspark, 2023).

2.3.1 Duration of rainfall (short duration and high intensity)

Rainfall intensity is defined as the empirical quantification of the degree of risk to which a landscape unit is subjected (Crepani *et al.,* 2004). Intense rainfall, or extreme rainfall, is also known as maximum rainfall and has an irregular distribution both temporally and spatially. As previously evidenced, these events cause significant damage, including soil erosion, flooding, economic losses, as well as impacts on reservoirs (Silva Neto *et al.,* 2016).

There are several methodologies for estimating short-duration and high-intensity rainfall. Among them, those related to intensity-duration-frequency (IDF) stand out, ideal for estimating the intensity of rainfall to be considered in determining flood flows. According to Back *et al.* (2012), IDF relationships are obtained through statistical analysis of long series of data observed in pluviographs .

Back *et al.* (2012) developed relationships that describe precipitation of different durations in the State of Santa Catarina, promoting the disaggregation of daily rainfall into short-term events. This resulted in the construction of series of maximum annual rainfall, with durations varying between 5 and 1440 minutes, based on records from thirteen rain gauge stations . In a similar context, Silva Neto *et al.* (2016) applied the Gumbel cumulative probability function fitting method to annual maximum daily precipitation data. This procedure allowed obtaining the intensity-duration-frequency equation, applied to 24-hour rain in the city of Guaraí, in the state of Tocantins. The results revealed a good fit of the model to the data series, with significance in the tests performed.

Dame *et al.* (2008) used synthetic option series to estimate IDF relationships. Among the most commonly used methods are those that are based on relationships between rainfall of different durations to disaggregate the maximum daily rainfall into rainfall of shorter duration. This method is advantageous due to its simplicity, the quality of the results and its applicability in different locations, giving it regional validity. In Brazil, the relationships between durations, published by CETESB (1986), are widely used, as well as the approaches by Mello *et al.* (2003), Ferreira *et al.* (2005), Soprani and Reis (2007) and Oliveira *et al.* (2008).

There are a variety of methods available for obtaining data on short-duration, high-intensity rainfall, and the choice of which method to use will depend on the specific characteristics of the region in question.

2.4 IDF equations

According to Pereira *et al.* (2007), hydrological studies require not only knowledge of the maximum rainfall recorded in historical series, but also the ability to predict the maximum rainfall that can occur with a given frequency. This forecast can be obtained from the analysis of observations of intense rainfall over a period of time that is sufficiently long and representative of extreme events.

Elements such as the design of rainwater drainage systems, spillways, protection structures against floods and water erosion are of great importance (Sobieraj *et al.*, 2022). Furthermore, it is essential to understand the three main quantities that characterize precipitation: intensity, duration and frequency (Barbosa; Fernandes, 2012).

The Heavy Rainfall Equation, commonly called the IDF Equation, is the main tool for characterizing the relationship between these quantities. Pereira *et al.* (2007) highlight that the annual maximum intensity series, for each duration, are adjusted to the distribution of extreme values, known as the Gumbel distribution :

$$F(X) = \exp^{-exp\left(\frac{X-\propto}{\beta}\right)}$$ **Equation (01)**

In which Fx is the Gumbel cumulative distribution and ∞and β are, respectively, the position and scale parameters.

Studies have been developed to determine IDF equations, such as Westra *et al.* (2014), Nyamathi and Kumar (2021) and Ortiz and Martínez- Graña (2023). To determine an IDF, it is necessary to analyze the density data of the rainwater network and the relationship to the short observation period available. This requires extensive work analyzing, interpreting and collecting large data sets (Martel *et al.*, 2021).

It is worth noting that, in Brazil, not all locations have IDF equations established. This makes carrying out studies on floods and other related events more challenging, precisely because of the difficulties in finding data that correspond to the profile of that region, basins, etc.

According to Moreira *et al.* (2020), in the state of Bahia, there are 20 adjusted equations that relate the intensity, duration and frequency of maximum precipitation for several municipalities and locations, including Barreiras, Brotas de Macaúbas, Cândido Sales, Carinhanha, Cocos, Ibipeba, Formosa do Rio Preto, Ipiaú, Itamaraju, Itapebi, Ituberá, Juazeiro, Medeiros Neto, Morpará, Salvador, Santa Cruz da Vitória, Santa Maria da Vitória, Rafael Jambeiro and Teodoro Sampaio.

Furthermore, Moreira *et al.* (2020) observe that the lack of information based on intense rainfall equations for most locations in the State of Bahia has led to the use of data from rainfall stations close to the locations where the projects are developed. However, this results in unreliable estimates due to the spatial variability of rainfall data.

2.5 Environmental Modeling

Environmental modeling represents an organized set of systemic elements and interactions (Christofoletti 2015; Bianchi; Campos, 2023). Also, according to the concept of Figueiras (2001), it refers to mathematical models created to represent characteristics or processes of the real world. These models aim to increase knowledge about a process, predict values in observed areas and prove, or not, hypotheses made about the process.

For environmental analysis and modeling, it is important to distinguish these systems from the characteristics, whose action should seek to abstract said system from reality. Environmental modeling must consider the complexity of natural processes and the spatio-temporal interactions between the various variables that make up these systems (Oliveira, 2016).

Biological systems are often represented through models that can be innovative with various computational tools. These tools enable this interaction between man and the representation of nature, contributing to these biological processes being properly recognized.

There are several models and approaches applied to different geographic representations, and, according to Christofoletti (2015), there is a typology of models in hydrology that are used for different types and developed for different objectives. Thus, models can be classified into: a) continuous time or events; b) daily period; c) monthly period and annual periods, based on data availability for computational and management purposes.

2.6 Hydrological Model (HEC HMS)

According to Rennó and Soares (2002), hydrological models can be defined as a mathematical representation of the water flow and its constituents over some part of the Earth's surface and/or subsurface. There is an intrinsic relationship between hydrological modeling, biological and ecological flow, as the transport of materials through water is influenced by biological activities that can increase or decrease the amount of these materials in the water, and the water regime can affect different habitats.

Furthermore, hydrology is closely related to climatic conditions, and therefore hydrological and atmospheric models should be coupled. However, in practice, this integration becomes quite challenging, since atmospheric models work with much higher spatial resolutions than those used in hydrological modeling (Rennó; Soares, 2002).

Hydrological models aim to represent the terrestrial part of the hydrological cycle, transforming precipitation in a basin into flow in a given section of a river. These models can vary considerably, reflecting different typologies, depending on their objectives, which can be simulated or optimized (Almeida; Serra, 2017).

Regarding their genesis (hydrological cycle), these models can be empirical, conceptual or based on physical processes. Spatial discretization and architectures can vary from aggregated to distributed . Furthermore, time is a relevant dimension, with models aimed at simulating isolated events and others for continuous simulation (Almeida; Serra, 2017).

Hydrological modeling has been widely used as a tool to obtain deeper knowledge about the physical phenomena involved and to predict scenarios. They comprise systems of equations and procedures composed of variables and parameters that are increasingly present in environmental studies, helping to understand the impact of changes in land use and preventing future changes in ecosystems (Almeida; Serra, 2017).

Oliveira (2016) states that, although there are different types of models available, their classification must consider that there is no superiority of one model over another, but rather its applicability due to the analysis of the aspects.

Furthermore, the use of hydrological models in environmental planning is broad, as it has variables that will determine the modeling carried out, such as, for example, sizing, real-time forecasting and assessment of land use; flood sizing and forecasting; calculation of reservoir volume, groundwater level; river-aquifer interaction; simulation of system changes; effects of downstream runoff, tributary impact, reservoir eutrophication, water supply and treatment network; irrigation and river navigation network (Oliveira, 2016).

2.7 HEC RAS Hydraulic Model (Modeling - 1D and 2D)

The Hydrological Enginnering Center - River Analysis System (HEC-RAS) is software that performs mathematical modeling, developed in the early 1970s, widely recognized for its ability to perform one-dimensional (1D) modeling (USACE, 2002).

According to Leitão (2018), over time, the ability to perform two-dimensional (2D) hydrodynamic modeling for non-steady flows was added to HEC-HAS, using Saint-Venant equations or diffusion wave equations .

For non-steady and non-uniform flow for a one-dimensional open channel, the Sainte-Venant equation is based on two laws of physics, the principle of conservation of mass and the principle of conservation of momentum, as described by Bruno *et al.* (2021) in the following equations:

$$\frac{\partial A}{\partial t} + \frac{\partial (uA)}{\partial x} = 0 \qquad \textbf{Equation (03)}$$

$$\frac{\partial Q}{\partial t} + \frac{\partial Qv}{\partial x} + gA\left(\frac{\partial z}{\partial x}\right) + s_f = 0 \quad \textbf{Equation (04)}$$

Where At is the total area of the section, Q the flow rate, qa additional lateral flow per unit length, g is the acceleration of gravity, A is the wetted area, dz / dx is the slope of the waterline , sf is the terrain friction slope (Bruno *et al.*, 2021).

The 2D area, located on the HEC-RAS taskbar, can be used in several ways. In this study, it will be used to perform detailed 2D modeling of the channel and flood dam.

According to Leitão (2018), 2D modeling is achieved by adding 2D flow elements to the model, in a similar way to including a storage area. This 2D area is added by drawing a polygon, developing the computational mesh and connecting the 2D model with 1D elements, applying the appropriate boundary conditions.

With this software, it is possible to simulate and perform analyzes involving permanent and non-permanent flow, water quality analysis and sediment movement, which allows the user to obtain very accurate information in different types of simulation (ANA, 2018).

The transient flow modeling option is made available by the Unsteady algorithm NETwork Model (UNET) in HEC-RAS versions from 2000, version 3.0. In HEC-RAS, it is possible to calculate subcritical, supercritical and mixed flow regimes, allowing transitions between them. However, it is necessary to apply the LPI (Local Partial Inertia) technique to reduce numerical instabilities due to discontinuities in the flow, although this may result in some loss of precision in the results (Oliveira, 2016).

It is important to highlight that the information inherent to boundary conditions and flows are defined in the HEC-RAS program itself, not which slope, runoff, depth and design flow parameters are inserted according to each situation (Reis; Schmidt, 2017) .

2.8 Risk Assessment and Estimation

According to Diginino and Carpi (2007), the term “risk” is associated with susceptibility, vulnerability, sensitivity or potential damage, representing the probability that an expected or unexpected event will become a reality. Daginino and Carpi (2007) also identified several categories of rich people's risks such as: natural risks, which correspond to those that cannot be easily attributed or related to human action, although some indirect actions can influence them. In addition, there are other risks such as technological, social and environmental. The latter, environmental, is the result of the association between endogenous risks and risks arising from natural processes aggravated by human activity and the occupation of the territory.

Brito and Oliveira (2016) also conceptualize risks as being “results of adverse events, natural or man-made, on a (vulnerable) ecosystem, causing human, material and/or environmental damage and consequent economic and social losses”.

As an example of environmental risks, we can mention what happened in the mountainous region of Rio de Janeiro in 2011, when one of the biggest natural disasters related to the mass movement and floods resulted in 947 fatal victims, 300 disappearances, more than 5,000 people homeless and reaching approximately 1 million people (Brito; Oliveira, 2016).

With the system to manage risks, these consequences can be mitigated, since alerts can be given when the possibility of occurrence is estimated. Risks can be used to explain cause and effect both on a macroscale, such as in the use of the river basin, or in a metropolitan region, and on a microscale (Diginino; Carpi , 2016).

Figure 1 shows the number of deaths that occurred in Brazil in the year 2022, it can be seen that in that year, there were more than 450 victims.

Figure 1. Deaths from excess rain in Brazil

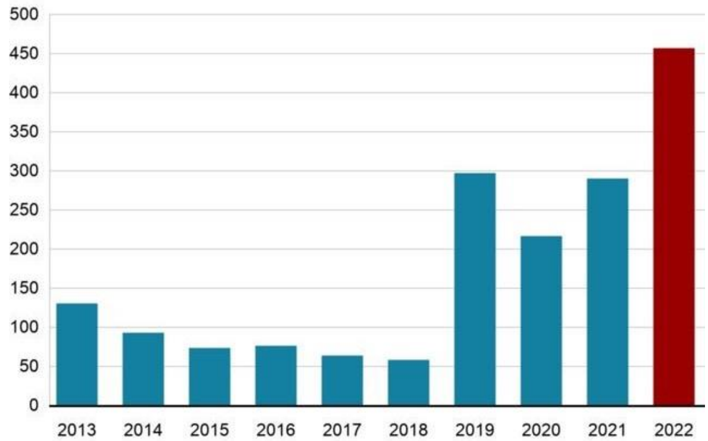

Source: BBC (2022)

In line with the threats previously highlighted, Oliveira (2018) presents an approach that assesses both the risk and the threat, which was used as one of the parameters of this study.

R = P(fA) * C(fV) * g-1 **Equation (05)**

Where R corresponds to Risk; o P the probability of a physical event or danger occurring (A), causing consequences C (which may be to people, goods and/or the environment), depending on the vulnerability V of the exposed elements, and which can be modified by the degree of management g. This study focuses on the analysis of "P" and "C", as modeling will make them visible, as well as the consequences faced by the region.

Festa *et al.* (2022) carried out studies of flooding and its economic impacts on a microscale, in Southern Italy using the Risk equation:

$$R = H \times V \times E$$ **Equation (06)**

Where R is the total value of Risk; V expresses the adverse effects suffered by vulnerable people and structures; E exposure of the elements at risk and finally the H consequence of the impact of a dangerous event (danger of a natural event).

In the case of flood risk, the assessment generally involves consideration of spatially distributed flood levels over probabilistic time. Recurrences of events of a given magnitude are often used to estimate the potential for exposure to flood hazards. On the other hand, vulnerability focuses on assessing the potential degree of damage that exposed elements may suffer, based on estimates of flood depths (Festa *et al.,* 2022).

2.8.1 Flood Risk

To understand the risk of flooding, it is important to bring its concept and the difference between flash floods, floods and flooding. According to Tucci (2007), flooding in urban areas is a chronic problem that dates back to the beginnings of cities and urban agglomerations. These events occur when the waters of rivers, streams and rainwater drainage systems exceed their transport capacity, overflowing into areas that are normally used by the population for residential, transport, leisure, commerce, industry and other purposes.

Flooding can also be characterized as high-speed, high-energy surface runoff, caused by intense and concentrated rainfall in a short period of time, normally in small basins with rugged relief. It is characterized by the sudden increase in flows in a certain drainage and sudden overflow of the river channel (Brasil, 2012).

Regarding floods, Tucci (2007) categorizes them into two types: floods due to urbanization and floods in riverside areas. Urban flooding occurs due to the increased frequency and magnitude resulting from urbanization, which involves the development of areas with impermeable surfaces and inadequate drainage systems, as well as obstructions such as embankments and bridges. Floods in riverside areas are natural and affect the populations that inhabit the alluvial barriers of rivers, being triggered mainly by natural processes in which rivers occupy their largest barriers, generally in extreme events with an average return time of around 2 years.

Finally, flooding is characterized by occurrences in flat areas, depressions or valleys, in which surface runoff is hampered by topography and the absence or insufficiency of drainage systems in urban environments. Furthermore, there is a lack of green areas and reduced infiltration in the soil situated for surface runoff, limiting the assistance that could be provided by suspended aquifers to mitigate these occurrences (Teodoro; Nunes, 2007).

In figure 2, we can distinguish between flooding, flooding and flooding, noting that there are situations considered normal, but these events can turn into natural disasters.

Figure 2. Representation of flooding, flooding and inundation phenomena

Source: Garcia (2021)

According to Hora (2009), floods represent one of the most common natural phenomena in the world, affecting numerous populations on all continents. They cause disastrous impacts in the affected areas, causing human and material losses. In 2007 alone, floods affected more than 164,662,775 people worldwide, causing a tragic loss of 8,382 lives. The author also states that floods have also caused major disasters for the Brazilian population, mainly due to the disorderly occupation of the riverbeds and the waterproofing of the soil in urban basins (figure 3).

Figure 3. Impact due to disorderly urbanization

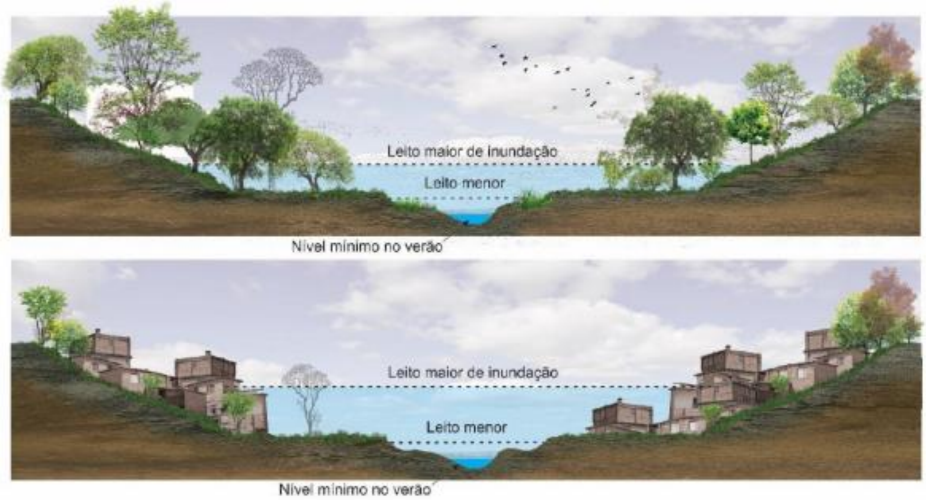

Source: Benini (2017).

The lack of flood monitoring and control policies has increased damage and losses in cities. This increase is due to the lack of adequate urban planning, the lack of knowledge of the risks associated with flood-prone areas and the lack of initiatives to resolve this problem (Hora, 2009).

Figure 4 shows the number of natural disasters that occurred between 1990 and 2020, making it possible to identify that the population was most affected by hydrological disasters followed by meteorological disasters.

Figure 4. Number of cases of natural disasters in the world between 1990 and 2020.

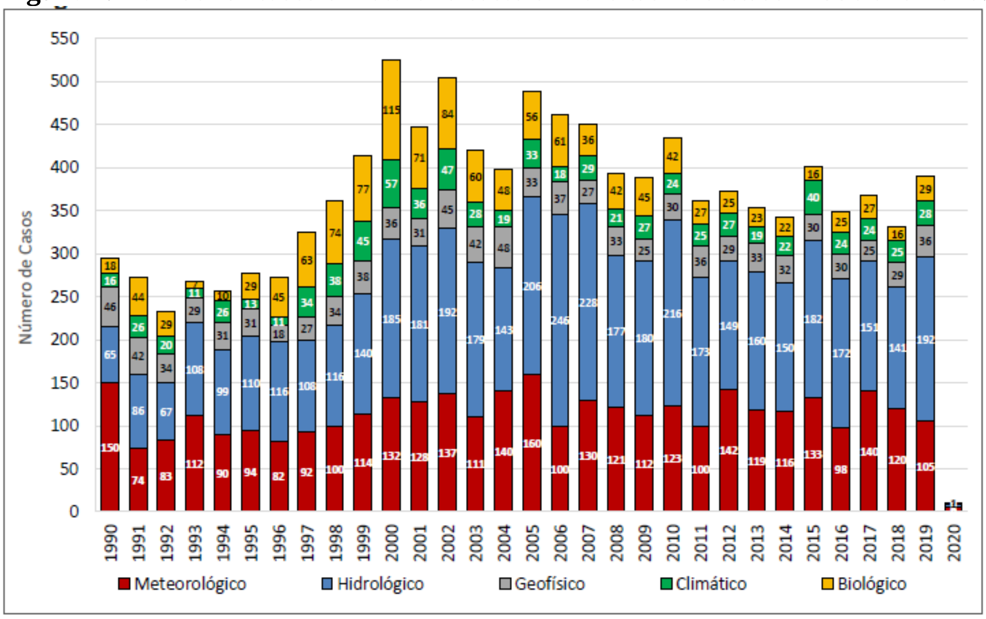

Source: Garcia (2021)

It is important to highlight the difference between disaster, damage and loss. According to Siqueira (2017), disaster is the result of adverse events, natural or man-made, on a vulnerable system, causing human, material and/or environmental damage, and consequent economic and social losses. The intensity of a disaster depends on the interaction between the magnitude of the event and the vulnerability of the system and is quantified in terms of damage and losses.

Damage is a measure of the intensity or severity of the injury resulting from an adverse event. It is also defined as the intensity of human, material or environmental losses that occur as a consequence of a disaster (Araújo, 2012). Flood damage can be classified as tangible or intangible. Tangible damages are those that allow a monetary expression, while intangible damages are those whose estimation of the associated loss is very difficult or even impossible (Jonov *et al.*, 2013).

To control and mitigate these flood risks, there is a protection system made up of a series of logical actions designed to reduce the impacts of flooding. Risk management emerges as a well-defined procedure for dealing with environmental or human-caused disasters, with floods being a representative example (Siqueira, 2017).

According to the author, risk management, based on the concepts of threat, exposure and vulnerability, can be conceptualized and approached in five stages: diagnosis, preparation, prevention, management of adverse events and recovery.

2.9 Economic Reasons

The open market in the city of Catu is extremely important for the local population. Through it, there is an economic rotation of the products that are sold there, benefiting not only urban residents, but also those in rural areas, as they sell their products such as vegetables, fruits, as well as products of animal origin.

Residents of the areas surrounding the fair are frequent buyers of the food sold, as their proximity facilitates access. Furthermore, the fair attracts people from neighboring municipalities, such as Pojuca and São Sebastião do Passé, who come to participate in local commerce. In other words, the commercial warehouse plays a significant role in the economy, boosting the activities of small producers and micro-entrepreneurs. This, in turn, stimulates job creation and income distribution in the region. Furthermore, the phenomenological dynamics of the fair promote meetings between people who, in other situations, would not know each other.

However, it is important to highlight that the occurrence of floods can interrupt this flow of people, resulting in economic losses, as shown in figure 5.

Figure 5. Economic losses caused in Brazil by floods between 1990 and 2019.

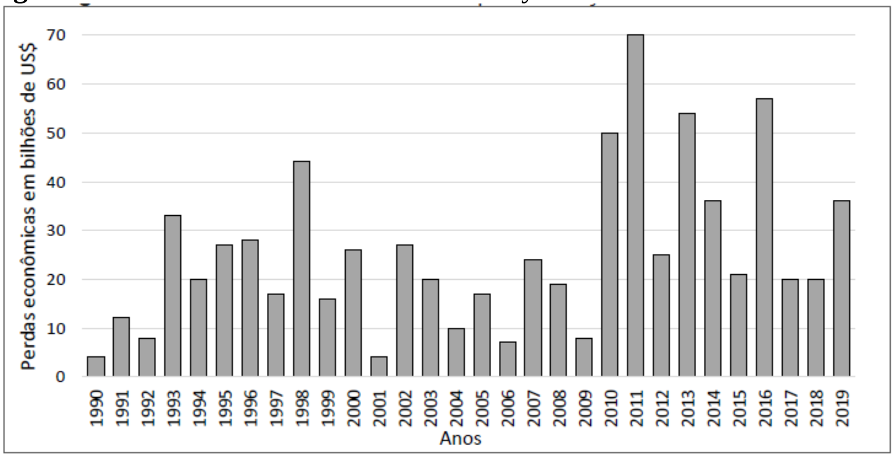

Source: Garcia (2021)

2.9.1 Economic Indicators

According to Lourenço (2002), economic indicators (IEs) essentially represent data or information that indicates or points to the performance (individual or integrated) of the different variables and phenomena that make up an economic system, whether at the level of a country, region or state.

According to the author, these IEs are fundamental both to provide a better understanding of the current situation and the outline of short-term trends in the economy, and to support the strategic decision-making process of public (government) and private agents (companies and consumers).

Araújo and Ribeiro (2018) emphasize that street markets bring benefits to the local economy, generating income that, for the most part, goes to urban commerce. However, this type of economic indicator often goes unnoticed by municipal bodies, receiving little attention and incentives. In other words, the interference of this economic development by floods compromises the municipality's revenue from activities derived from commerce.

Assisi *et al.* (2006) carried out a study on the impact of fairs in Jequitinhonha Minas Gerais and observed the impacts that free fairs have on some cities in this region, such as a 50% increase in sales in urban commerce on fair days, with more significant in establishments for direct food consumption, such as bakeries, cafeterias, bars, as well as hairdressing salons.

It is important to highlight that the volume of expenditure in urban commerce exceeds the revenue obtained at fairs by around 80% of the total received. Even in fairs in small municipalities, where the movement is initially small, there are real impacts on local commerce and the income of market traders. This demonstrates effective dynamism in the economy of these municipalities (Araújo; Ribeiro, 2018).

3 MATERIALS AND METHODS

3.1 Characterization of the study area

According to the Brazilian Institute of Geography and Statistics (IBGE, 2023), the territory where the municipality of Catu is located today was inhabited by Pataxó and Tupiniquin Indians, forming part of the land of Sesmarias do Conde da Ponte, where numerous settlers flocked at the time. The settlement of these settlers began in 1872, resulting in the administrative division consisting of three districts: Catu, São Miguel and Sítio Novo (IBGE, 2023).

Currently, the municipality of Catu has approximately a territorial area of 426, 955 km² and is located around 70.13 km from Salvador, capital of the State of Bahia (Figure 6). Its population is estimated at 55,222 inhabitants, with a demographic density of 122.72 inhabitants /km².

Figure 6. Location map of the municipality of Catu, Bahia (Brazil).

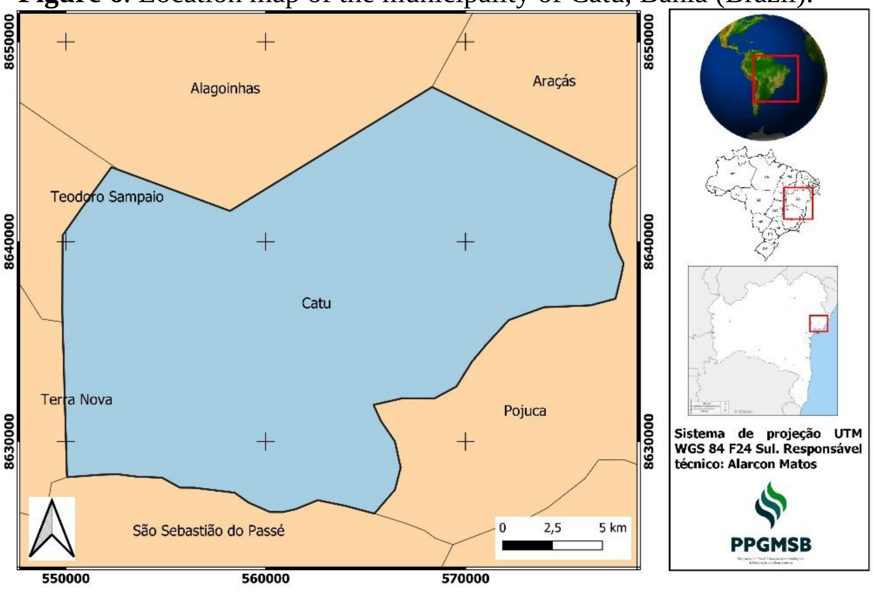

Source: Alarcon Matos de Oliveira, 2023.

Quiricó Pequeno rivers, in addition to the Pojuca river that limits the municipality with that of São Sebastião do Passé (Menezes, 2011). The predominant vegetation in the municipality of Catu is dense rainforest, although high temperatures, with an average of 25ºC, and high rainfall are distributed throughout the year, the dry period can vary from 0 to 60 days (Menezes, 2011; EMBRAPA, 2010).

Borges (2015) describes the climate in the municipality as humid to sub-humid , with a water index of 0% to 20%, a water surplus between 50 mm and 300 mm and with rainfall concentrated in the autumn-winter period, with an average annual temperature of 23.9°C. As for rainfall, when heavy rains occur, especially in the region of the city's Supply Center, located in the Santa Rita neighborhood, the area becomes flooded, preventing pedestrian and vehicle traffic, significantly harming stallholders and the development of local commerce. and the general population.

According to data from IBGE (2022) on the professional occupation profile, the average monthly salary is 2.7 minimum wages, although only 15.3% of the population are part of the Economically Active Population (EAP), totaling approximately 8,388 people, thus indicating a concentration of income. Compared to the past decade, the percentage of the population with nominal monthly per capita income was up to ½ minimum wage in 2010. However, the schooling rate for 6 to 14 year olds in 2010 was 93. 7%. In the following years, the Basic Education Development Index (IDEB) achieved was 5.1 in the initial years (equivalent to 98.1%) and 3.9 in the final years, demonstrating progress in terms of education compared to the previous decade. previous.

3.2 Materials

To obtain the results of this research, topographic data from the area was collected and the 30 m Shuttle Radar Topographic Mission (SRTM) was adopted, which is the digital model of the terrain.

Hydrological modeling was conducted using HEC HMS software. The process involves delimiting the basin and sub-basins, carried out with the aid of QGIS 3.16.13 software, as well as soil characterization and analysis of occupation in the basin.

For the two hydrological and hydrodynamic models in question, the return times needed to be well defined in order to obtain the results.

3.3 Methods

This study used the hypothetical-deductive method, which is based on the identification of problems, gaps or contradictions present in prior knowledge or in already conditional theories. From these problems, conjectures, solutions or hypotheses are formulated. Subsequently, these assumptions go through an evaluation process, called the falsification technique (Diniz, 2015).

Within this context, falsification can be carried out through several approaches, including experimentation and statistical analysis. After analyzing the results, previously elaborated conjectures, solutions or hypotheses are evaluated, which can be reputed (rejected) or corroborated.

3.3 Characterization of the Catu River Basin

The hydrological characterization of the Catu river basin was carried out, whose climatological reference station is located in the city of Alagoinhas. Climatological data from the city of Alagoinhas were used as a primary source, due to the lack of a climatological station in Catu, which is the place of interest.

According to Porciúncula *et al.* (2016), the region has around 140,000 inhabitants, who live in an area of 1179 km², located around 107 km from the capital, Salvador.

This basin has a developed surface drainage system, with perennial rivers and some remaining lakes. The average annual rainfall reached 1,234.1 mm, while the actual evapotranspiration is 1,096.2 mm (Figure 7). These data resulted in a water surplus of 137.9 mm/year, according to the Energy Information System (SEI) in 1999, showing the relevance of these characteristics for understanding the region's water dynamics (SEI, 1999).

Figure 7. Average monthly accumulated rainfall for the Alagoinhas region

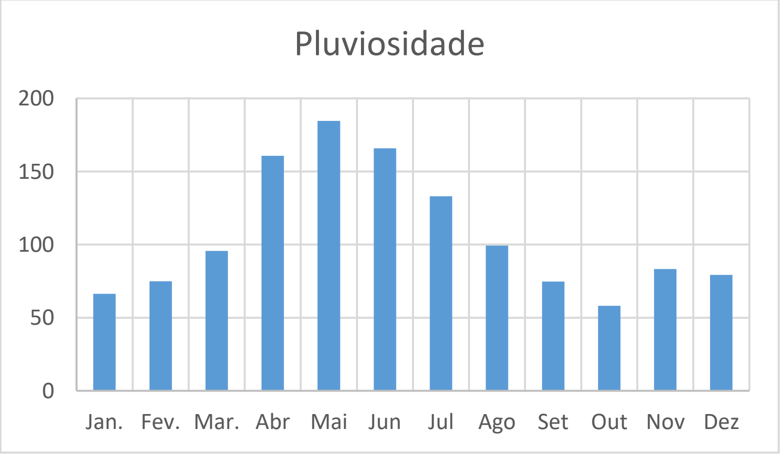

Source: INMET – Climatological normals from 1991-2021

According to Porciúncula *et al.* (2016), the municipality of Alagoinhas stands out in the geoenvironmental and hydrogeological sphere for housing an important underground water reserve called the São Sebastião aquifer. This reserve covers most of the region, often overlapped by the Marizal Formation , which in turn plays a crucial role in protecting this source.

Still according to its water balance, there is a tendency for water deficit in the spring to summer periods, with water replacement returning in April (Figure 8). It is important to note that this period also coincides with the most favorable season for frequent rains that cause flooding in the studied region, although the phenomenon can occur in other periods due to the anthropization of the region.

Figure 8. Water Replacement

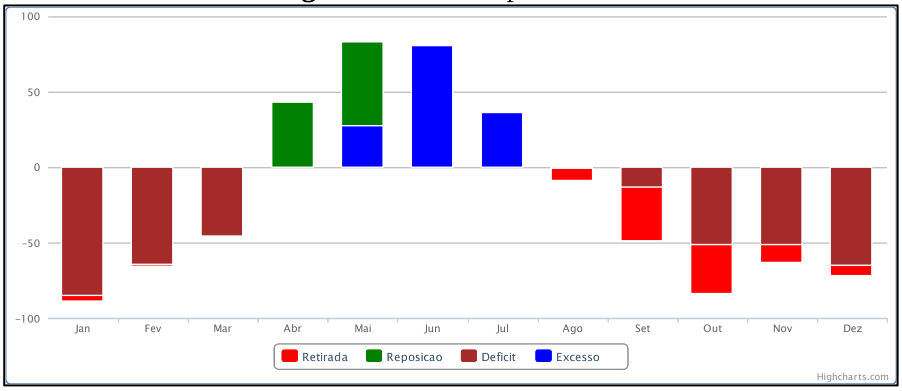

Source: INMET – Climatological standards from 1991-2021

3.3.1 Characterization of Land Use and Cover

The river basin under study, in general, is described by a predominance of land uses, including pastures, forestry areas, forest fragments and small urban centers. The exception to this description is the city of Alagoinhas, which stands out as a medium-sized municipality. This distribution of land use and coverage can be seen in Figure 9.

Figure 9. Land Use and Cover Map

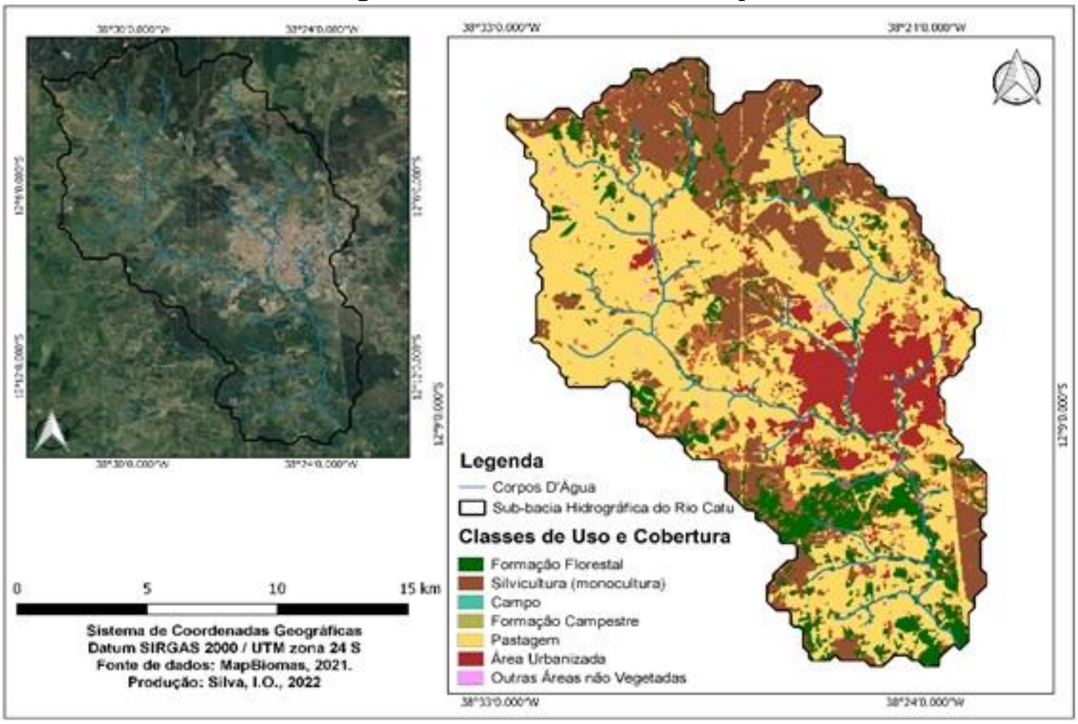

Source: Alarcon Matos de Oliveira, 2022.

3.4 Determination of the Hyetogram

To carry out the modeling of the flood profile of the City of Catu in this study, it was necessary to follow a sequence of steps in a synchronized and well-defined order. The first step is to define the IDF equation that best fits the research carried out in question. In this sense, the IDF equation used was based on the model proposed by Moreira *et al* (2020). The IDF equation is represented by:

$$IDF = \frac{K.TR^2}{(t+b)^2} \quad \textbf{Equation (02)}$$

Where, IDF – represents the intensity, duration and maximum frequency of precipitation, mm h^{-1}; TR – return period in years; t – precipitation duration, min;

After obtaining the maximum precipitation values for each duration and return period, the parameters (K, a, b and c) of the IDF equation were adjusted. Where:

K = 829.668

a = 0.1666

b = 12.856

c = 0.777

Where: K and a are empirical parameters of the IDF equation, and TR the return period, in years where: i = estimated intensity; t = time in minutes and b and c = adjusted empirical parameters. Therefore, the following adjusted parameters were used based on the local rainfall data for the IDF constants:

$$\mathrm{I} = \frac{K\,829.6680\ .\quad TR^{0.1660}}{= (t+B8)^{0.776}} \qquad \textbf{Equation (07)}$$

According to the methodology of Moreira *et al.* (2020), the adjustment of the parameters of the IDF equation was performed through nonlinear multiple regression, using the nonlinear Generalized Reduced Gradient (GRG) interaction method. The quality of adjustment was assessed based on the coefficient of determination (R^2). Furthermore, the assessment of data fit is carried out through regression analysis of observed data and estimated data, paying attention to the angular coefficient of the straight line. All these steps were carried out with the help of the Solver tool package for Microsoft Excel.

To obtain the desired results, it was necessary to determine the duration of the rains in minutes. It was decided to adopt a duration of 60 minutes, corresponding to the rainy period, with 5-minute intervals for each block. This approach allows for an adequate representation of the temporal variation of rainfall throughout the event.

Rain intensity was expressed in millimeters per hour and was calculated based on the mentioned IDF curve. In this way, it was possible to determine the accumulated precipitation over the period considered.

The alternating blocks methodology was adopted, recognized for its simplicity and critical importance in the research approach. This method proposes the disaggregation of rainfall totals into time intervals discretized by their total duration. From the total accumulated increments of precipitation, transformed into rain height, the blocks obtained are rearranged in a sequence such that, in the center of the rain duration, the largest block is located and then the other blocks, in descending order, one to the right and the other to the left of the larger block, alternately (Abreu *et al.*, 2017).

The alternating block approach is used to obtain a more realistic representation of the rainfall patterns observed in the study area in question. This technique consists of inserting the highest intensity peak and alternating the remaining values to get closer to the reality of rain phenomena (Figure 10).

Figure 10. Variation in infiltration speed over time.

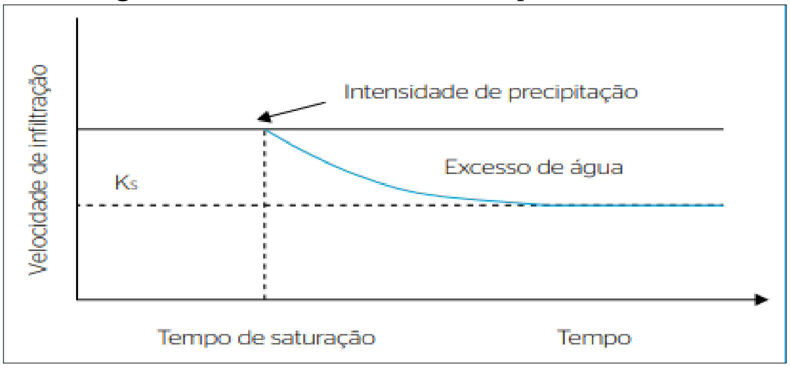

Source: Abreu, Sobrinha and Brandão (2017)

This graphic representation is extremely important for understanding the temporal distribution of intense rainfall throughout these periods and helps in planning risk mitigation and adaptation measures for extreme events (Abreu, Sobrinha and Brandão, 2017).

The hyetogram was generated based on data obtained in the study by Moreira *et al.* (2020) and inserted into an electronic spreadsheet that uses the Alternating Blocks methodology.

3.5 Determination of Return Times

To construct the hyetograph and hydrograph , defined return times were adopted, including periods of 10, 25, 50 and 100 years. These selected turnaround times are significant as they are not far off and not difficult to achieve.

They provide a suitable representation for analysis and study, allowing a comprehensive understanding of hydrological events. Considering these return times is essential to evaluate the behavior of the hydrological system in different scenarios and make informed decisions regarding the planning and management of water resources.

3.6 Determination of the Hydrograph in HEC - HMS

To determine the hydrograph, it was necessary to follow some steps. To determine land cover and use, the Mapbiomas classification was used , which is a collaborative network that seeks to reveal the transformations of the Brazilian territory through science, with precision, agility and quality, and make knowledge about land cover and land use.

This information is fundamental for the conservation and sustainable management of natural resources and for combating climate change (Mapbiomas, 2023).

For this study, collection 7 was used, where the classes were aggregated according to the respective colors of this collection, according to the report generated with the data entered in QGIS 3.16. (Figure 9). This figure highlights the land coverage and use of the river basin referenced in this study. They were grouped into 5 classes: forest, non-forest natural formation, agriculture, non-vegetated area and water body.

To characterize the soil, the Embrapa classification was adopted, considering that the soils in the region fall into the category of Red-Yellow Argisols (PVA). These soils are developed from crystalline rocks of the Barreiras Group and have a clay accumulation horizon, textural B (Bt), with yellowish-red colors due to the presence of a mixture of iron oxides hematite and goethite .

The construction of the hydrograph involved several steps, all directed towards discovering the Curve Number (CN), which provides data for the HEC HMS, including soil sealing. The HEC HMS is composed of three components: the Watershed Model, the Meteorological Model and the Control Specifications (USACE, 2008).

To process the hydrological model, it was initially necessary to insert data related to the river basin, as well as meteorological data. After data entry, methods were selected for calculating losses, rainfall-runoff transformation, composition of base flow and propagation in rivers. The choice of these methods took into account a variety of parameters, including sub-basin area, concentration time, infiltration factors and evapotranspiration.

Curve Number – Soil Method was adopted Conservation Service (CN-SCS), a rain-runoff model that consists of an empirical approximation between a given rain event and the surface conditions of the river basin to estimate direct surface runoff (Q) or runoff. It was originally developed to estimate the direct surface runoff (Q) generated in a basin or contribution area, estimating the potential water storage in the soil based on the adoption of a parameter known as Curve-Number (CN) . This parameter reflects the conditions of the vegetation cover, the physical-water attributes of the soil and the antecedent humidity, which is estimated based on the precipitation that occurred in the last 5 days (Alves, 2016).

Considering that the studied basin has three sub-basins, it was necessary to calculate the total area, length of the main river, highest point, lowest point, difference between the high and low point, slope, concentration time and delay time (Frame 1).

Frame 1. Physical characteristics of the basins**.**

PHYSICAL CHARACTERISTICS OF THE BASINS	**SUB-BASINS**		
	SUB1	**SUB2**	**SUB3**
Total area (km2)	118.75	83.21	189.62
Length of the main river (km)	23.45	16.42	29.76
Highest point (m)	330.00	245	111
Lowest point (m)	112.00	108	58
Difference between high and low point (m)	218.00	137	53
Slope (km)	0.009296375	0.008343484	0.001780914
Concentration time (sec)	8.025095802	6.248112522	13.16619006
Delay time (sec)	4.815057481	3.748867513	7.899714036

Source: Author (2023)

To reproduce the hydrograph in a section of the river, the concentration time was considered, constituting a hydrological parameter of great importance, as it informs the moment of occurrence of the maximum flow and the shape of the hydrograph (Farias Junior *et al.*, 2011). Winkler *et al.*, (2009) defines concentration time as the time required for the entire watershed area to contribute to surface runoff in the outlet section .

For the characteristics of the basin under study, the methodology proposed by Temez (1978) was adopted, which considers the basin with a maximum of 3000 km² and uses the following equation:

$$t_c = 0,3 \,.\, \left(\frac{L}{I^{0,25}}^{0,76}\right) \quad \textbf{Equation (08)}$$

Where:

t_c– concentration time (h);

L – length of the main thalweg (km);

I – equivalent average slope (m/m).

By using the formula and considering the classes: water, urbanization, agriculture, dense vegetation and low vegetation, it was possible to calculate the curve number (CN) (frame 2). This step plays a crucial role in advancing the floodplain simulation, as the curve number reflects the soil's ability to absorb rainwater.

Frame 2. Number Curve Calculation

CLASS	AREA	AREA (KM2)	CN	A*CN
Water	101.44	0.101436	100	10.1436
Urbanization	27546.83	27.546828	90	2479.21452
Agriculture	283319.80	283.319799	78	22098.9443
Dense Vegetation	78534.90	78.534903	70	5497.44321
Vegetation pothole	500.19	0.500193	75	37.514475
SUM	390003.16	390.00		30123.26
			WEIGHTED CN	77.2385029

Source: Author (2023).

Based on this calculated value, it was possible to determine the amount of water that runs off the surface and, consequently, contributes to the formation of the flood zone.

It is important to highlight that this initial stage establishes the foundations of the hydrological model adopted in the simulation, allowing the understanding of the runoff and flooding processes. From that point on, appropriate methods were used to obtain the flood spot, providing a more accurate and detailed analysis of the flood scenarios in the study area.

Therefore, hydrographs and their influence on determining the floodplain are essential steps to understanding the hydrological behavior of the area under study and providing important support for the management of extreme events.

3.7 Determination of HEC flood spot

To obtain the flood stain, several steps were carried out. Firstly, it was necessary to define the geometry of the study basin, considering characteristics such as the relief and watercourses present in the region. Then, Manning roughness coefficients were used, which were pre-defined based on a database related to land use, in the HEC-RAS software. These coefficients are essential to calculate the resistance to water flow in different areas of the basin.

To achieve this, a simulation of a flood wave arising from an extreme precipitation event was carried out. We preliminarily noted the concentration time, which is fundamental in the formation of floods, causing difficulties in the movement of traders and residents, making it impossible to use this space as a supply center, in addition to economic losses due to the loss of goods.

The first attempt to carry out the modeling was in the one-dimensional (1D) model, but we highlight some errors, such as the constants that were adopted, as limitations of this research. Therefore, we chose to use a two-dimensional (2D) model for greater precision in determining the cross sections and to classify the Manning coefficient.

Boundary conditions, including flood elevations characterized by reference heights, were also considered to determine how far water can reach during a flood. Furthermore, hyetographs (hydraulic models) and hydrographs (hydrodynamic models) were used to simulate the behavior of water flow and, thus, determine the extent of the flood spot.

A Digital Terrain Model (MDT) with a resolution of 30 meters and a mesh of 12.5 meters was adopted in the numerical modeling, with the computational factor being the limiting factor as a smaller mesh was not used . These data are essential to accurately represent the relief of the studied region. The delimitation of the study area was based on the actual size of the city, ensuring that the simulation covered all relevant areas.

Once the simulation was generated, the flood patches were exported to QGIS software, allowing the creation of thematic maps detailing the areas affected by the flood event.

3.8 Quantification of economic losses

The present study used a simplified approach to obtain the economic losses resulting from floods in the municipality of Catu, based on the estimate of damage per downtime (DDP). This approach was incorporated into the damage quantification methodology of the present study, which weighted the damage in the flooded area according to the days of interruption of activities.

This damage is related to the impact on the local economy, representing the lost investment in employees unable to contribute due to the stoppage of activities in the municipality due to the floods.

Based on the duration of floods in the region, it is possible to quantify the damage associated with the days stopped. In this context, this study was based on research by Tachini (2010) and damages were estimated using the following equation:

$$DDP = \frac{LMI}{ND} . POP . DI$$ **Equation (09)**

Where:

DDP: damage related to the days of shutdown of the affected areas in reais (R$)

LMI: average weekly profit per individual (R$/week)

ND: number of days in the week

POP: number of people affected by the flood

DI: duration of the flood in days

4 RESULTS ANALYSIS

Hyetograms were presented, which graphically represented precipitation variations over time. The hyetograms were constructed using the techniques and data mentioned previously, allowing a detailed analysis of rainfall characteristics in different return periods.

Then, the flood patches resulting from the simulations were presented. Each return time was assessed separately, providing information on the extent and intensity of flood-affected areas. The results were presented in a clear and visually understandable way, through maps and graphs that highlighted the flooded areas in each scenario.

These results were of great importance for understanding flood risks and supporting decision-making related to urban planning, water resources management and reducing damage caused by extreme events. The analysis of hyetograms and flood spots provides a comprehensive view of the impacts of intense rainfall and assists in the implementation of preventive and adaptation measures in areas susceptible to flooding.

4.1 Hyetogram Analysis

Based on the alternating block methodology, hyetograms were generated with their respective return times, using the IDF equation presented previously, together with the variables extracted from the research carried out by Moreira *et al.* (2020).

$$Accumulated\ \mathrm{P} = \frac{Intensidade * duração\ \ (instante)}{Tempo\ total\ de\ duração\ da\ chuva} \quad \textbf{Equation (10)}$$

These calculations and methodological considerations are crucial for understanding and analyzing the spatial and temporal distribution of rainfall, which contributes to assessing the risks associated with extreme weather events.

The precipitation result indicates the amount of millimeters of rain that occurs every minute, representing a layer of water accumulated over time.

In figure 11 presented in the study, it is possible to visualize the resulting hyetogram for a return time of 10 years, followed by return times of 25, 50 and 100 years.

Figure 11. Resulting hyetogram for a return time of 10 years.

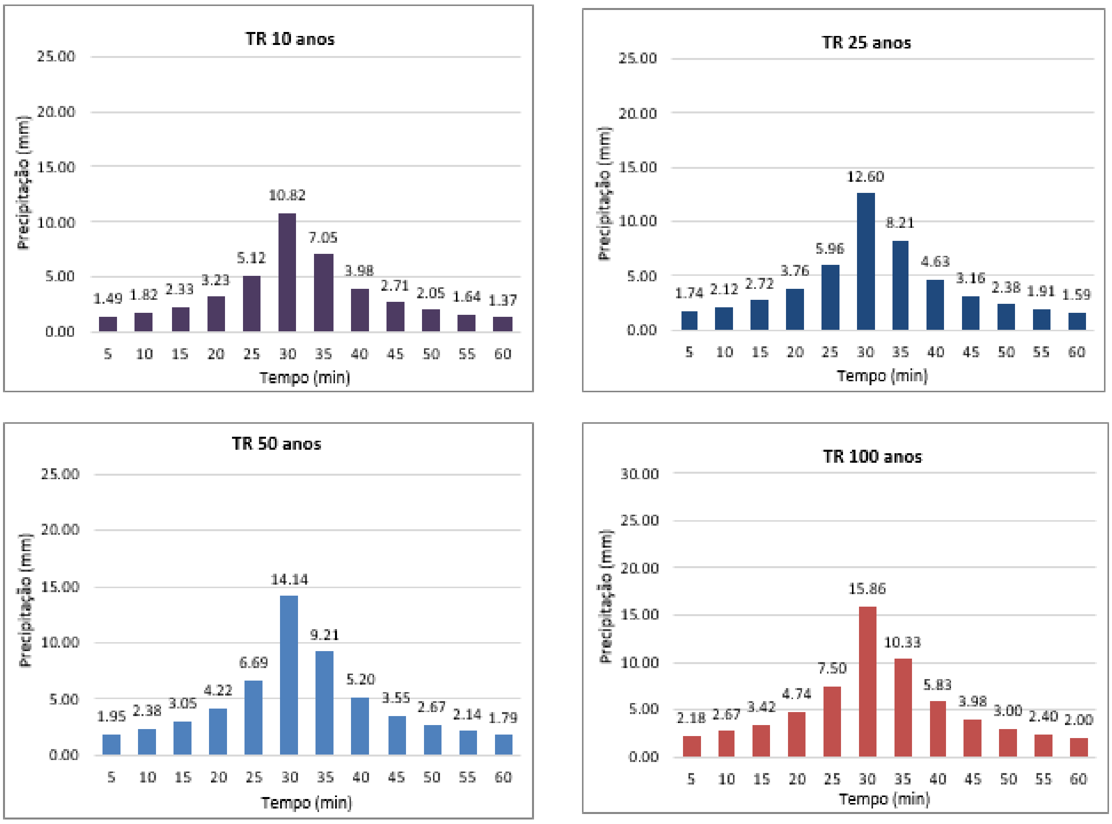

Source: Author (2023).

The figures provided show variations in turnaround times for events from different years. It is observed that, for a return time of 10 years, the precipitation peak reaches 10.82 mm. As the return time increases, the rainfall intensity also increases, reaching 12.60 mm at 25 years, 14.14 mm at 50 years, and 15.6 mm at 100 years, with the peak occurring at 30 minutes. After 35 minutes, the intensity begins to decrease, reflecting a common characteristic of rain.

The resulting hyetographs are valuable tools for infrastructure planning, water resources management and decision-making related to climate resilience.

4.2 Hydrograph Analysis

Hydrograph modeling involves combining the flows of the three sub-basins, resulting in a continuous line, as illustrated in Figure 11. The flow at junction 1 plays an important role in triggering floods in the study area, as it receives all the volume of water coming from the sub-basins.

Figure 12. Junction of the three sub-basins.

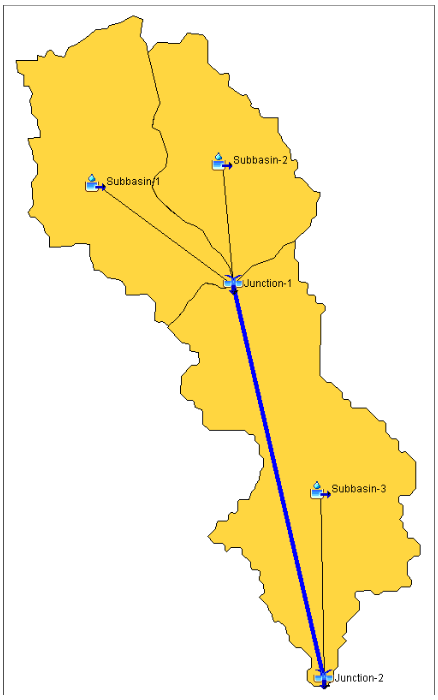

Source: Author (2023).

Rain peaks for return times are summarized in table 1.

Table 1. Rain peaks for return times

YEARS	PEAK
10	158 m³/ sec
25	250 m³/ sec
50	300m³/ sec
100	385m³/ sec

Source: Author (2023)

The hydrographs for the return times of 10, 25, 50 and 100 years were presented in table 2.

Table 2. Hydrographs for return times of 10, 25, 50 and 100 years.

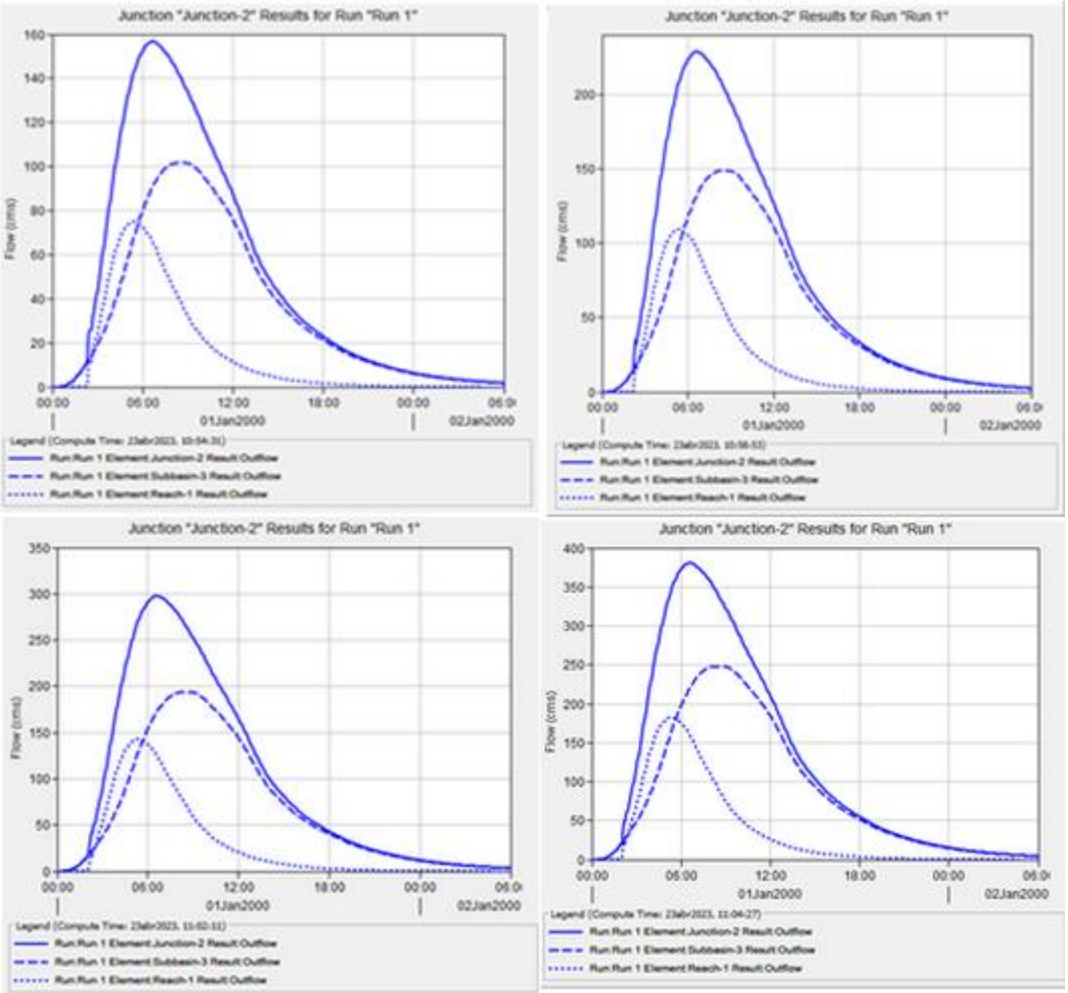

Source: Author (2023)

From the hydrographs obtained, it was possible to determine the floodplain of the studied area. These hydrographs play an important role in defining the flow of the region, taking into account the selected return time. It is observed that the return time of 100 years presented the highest rainfall, indicating intense rainfall and a greater potential for flooding.

Using hydrographs , it is possible to observe a continuous growth in flows as return times increase, all expressed in cubic meters per second. This analysis allows us to understand how flows behave and intensify in response to events of greater magnitude. This information is crucial to assess flood risks and assist in planning mitigation measures, such as the adequacy of drainage systems and containment structures.

Hydrograph modeling and flow analysis contribute to a better understanding of hydrological processes and are fundamental for hydraulic engineering studies and water resources management.

4.3 Flood Spot Analysis

From the simulation carried out, it was found that the study area is subject to flooding due to water flow, which is clearly evidenced by the flood patch represented by the area in blue (Figures 12, 13, 14 and 15). Each figure corresponds to a specific return time, being 10, 25, 50 and 100 years.

Figure 13. Flood Stain for 10 year payback time.

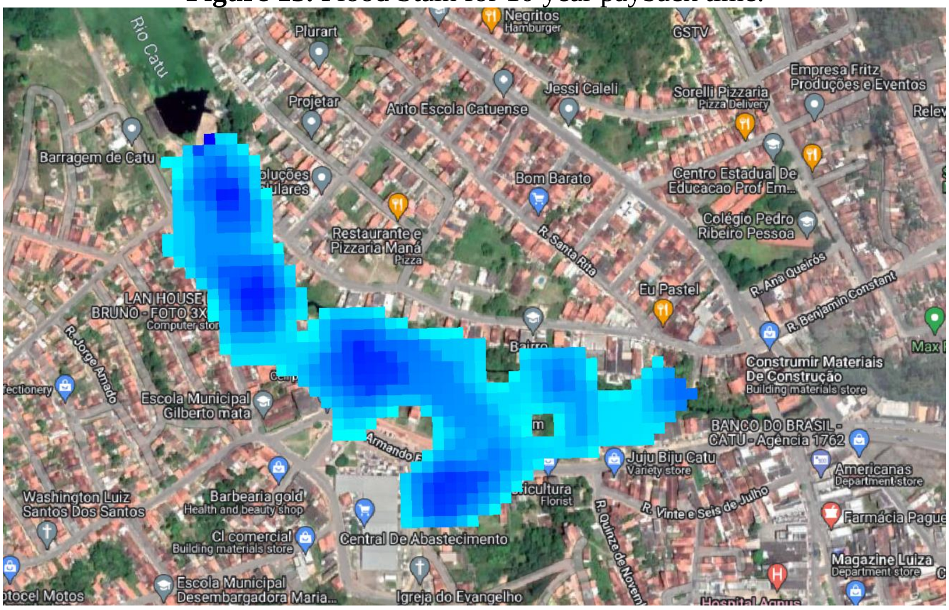

Source: Author (2023)

Figure 14. Flood Stain for 25 year payback time.

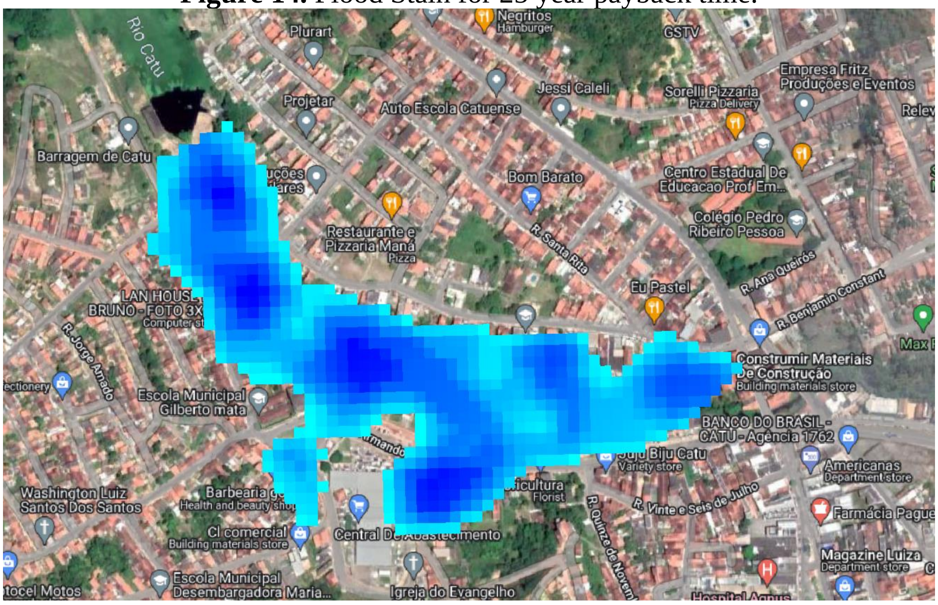

Source: Author (2023)

Figure 15. Flood Stain for 50 year payback time.

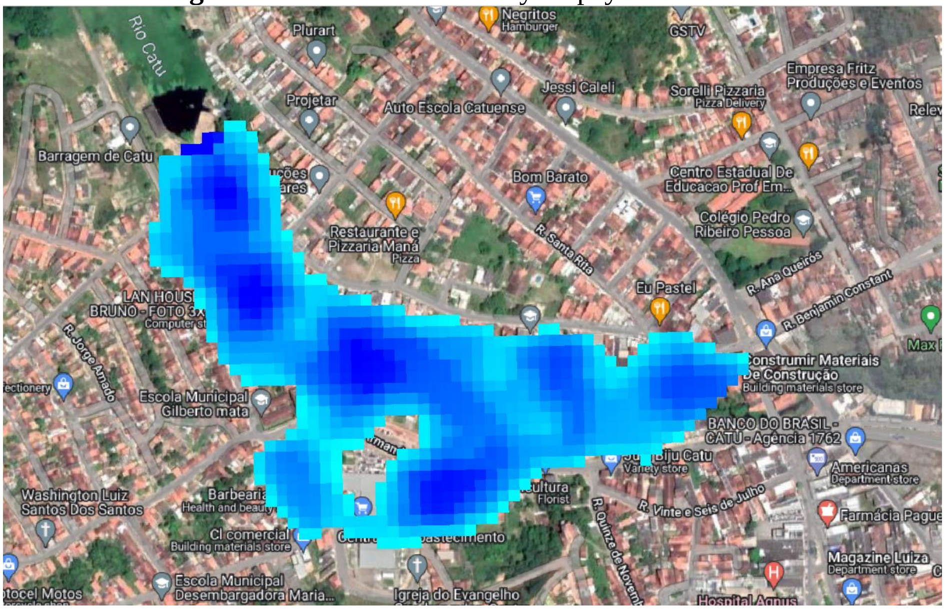

Source: Author (2023).

Figure 16. Flood Stain for 100 year return time.

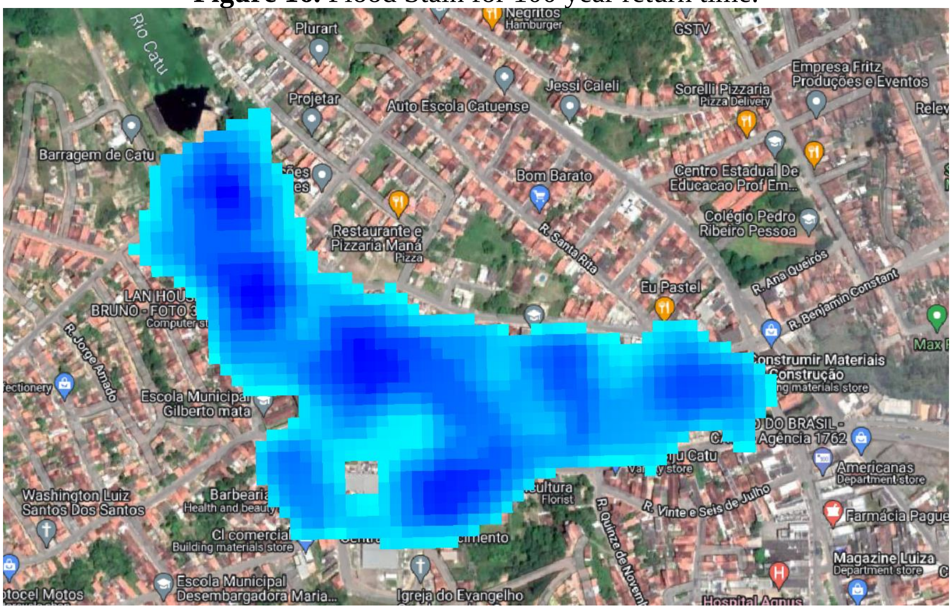

Source: Author (2023).

For a return time of 10 years, the results reveal a flooded area of approximately 89,000 m², with a maximum flood height of 4.23 meters, as shown in figure 12. Increasing the return time to 25 years, the flooded area expands to approximately 119,000 m², with a maximum height of 4.33 meters.

For return times of 50 and 100 years, a progressive increase in the flooded area is observed. The payback time of 50 years results in an area of approximately 140,000 m² and a maximum height of 4.62 meters. For the return time of 100 years, the flooded area reaches around 157,000 m², with a maximum height of 5.40 meters. Flood area and height data for return times were summarized in Table 3.

Table 3. Flood area and height for return times 10, 25, 50 and 100 years

Payback time (years)	Flooded area (m²)	Total height (m)
10	89000	4.23
25	119000	4.33
50	140000	4.62
100	157000	5.40

In general, when analyzing the different return times, it is possible to observe an evolution of the floodplain over time, with the floods becoming more evident and comprehensive. This information is crucial for understanding flood risks in the studied area and is useful for planning flood prevention and mitigation measures, as well as developing risk management strategies.

Figure 17 shows the rainfall recorded in the study area during the period of December 28, 2022. This image highlights the spatial and temporal distribution of rainfall in the region, allowing us to analyze patterns and variations over time. It is possible to observe the intensity and extent of areas affected by rain (Figure 17 and 18), providing important information for understanding the area's rainfall regime and for planning actions related to water resources, such as urban drainage and flood management.

Figure 17. Flooding in the Santa Rita neighborhood, Catu – BA

Source: Alagoinhas Notícias (2023)

Next, in figure 18, the Santa Rita neighborhood before the flood is shown.

Figure 18. Santa Rita neighborhood, Catu – BA.

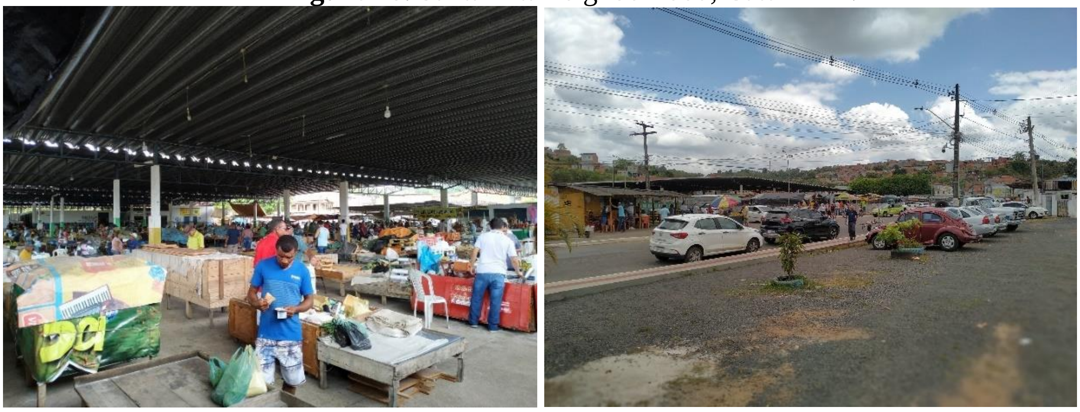

Source: Author (2023).

4.4 Analysis of the Logintudinal Profile and Cross Sections of the Flood Spot

Analysis of the longitudinal profile of the flood spot reveals the variation in water height along its course. This analysis made it possible to identify critical points and understand how flooding behaves across the terrain.

According to the longitudinal profile, the water variation for the four different return times showed the same characteristic at four points: at point A with coordinates x 1220881 and y 8625797; at point B, considered critical, the coordinates were x 1220908 and y 8625686; following respectively from point C, x 1221035 and y 8625604; and, finally, at point D, with the x axis of 1221125 and y 8625458.

In these specific areas, the water height analysis reveals the unfeasibility of the movement of people for local businesses, due to flooding. In cross-sections of the spot, this analysis provided *insights* into the spatial distribution of water and the extent of flooding at different points in the studied area.

Analyzing the points through modeling developed for a period of 10 years, one of the most critical locations close to the supply center is identified, noted by the intense concentration of water in the area in darker blue (Figure 19). The coordinates of this point are 1221126 on the x-axis and 8625471 on the y-axis, resulting in a considerable height of water.

Figure 19. Modeling performed for the 10-year layer

Source: Author (2023).

In the scenario analyzed in Catu, it is clear that the extent of the floodplain varies according to the different return times. For the return time of 25 years, it is possible to observe an increase in water concentration in relation to the previous return time, as shown in Figure 20.

Figure 20. Modeling carried out for the 25-year layer

Source: Author (2023).

For the period of 50 years, it can be seen that at the same point there is a concentration of water in lighter blue tones, however, in a significantly greater proportion than the previous return time (Figure 21).

Figure 21. Modeling carried out for the 50-year layer

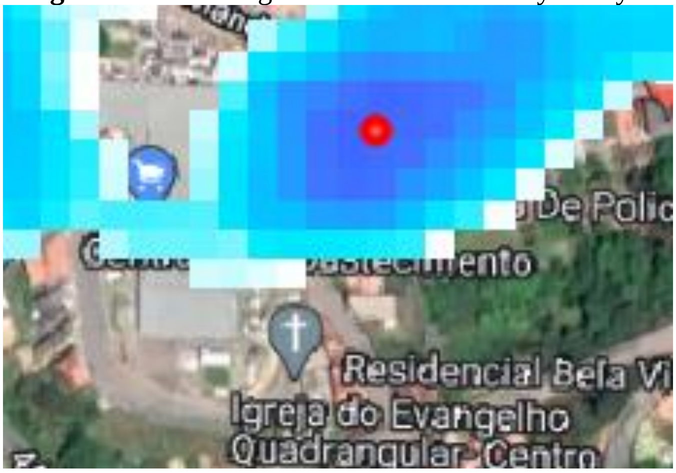

Source: Author (2023).

In the scenario of 100 years of return time, the situation worsens, to the point that the precise identification of the city's supply center becomes impossible due to the large volume of water, resulting in a total flood, as evidenced in Figure 22.

Figure 22. Modeling carried out for the 100-year layer

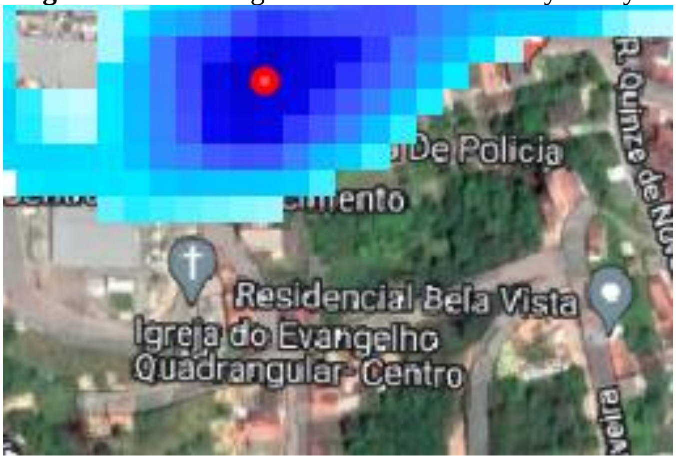

Source: Author (2023).

4.5 Loss Modeling

According to information provided by the current Catu Municipal Fair Coordination, around 200 vendors depend on the income generated by their merchandise. Each stallholder makes an average profit of R$250.00 per week. Considering the 200 stallholders, the weekly profit reaches approximately R$50,000.00. The importance of the fair's development in the city is evident, as it generates significant economic activity for both sellers and buyers.

The agricultural sector in the city of Catu is discussed in public events conducted by the local Federal Institute of Education, Science and Technology of Bahia, which offers courses focused on the area, such as the Agricultural Technician course. This contributes to the growth of open-air markets and brings innovation to family farming. The majority of market vendors live in the rural areas of the neighborhoods, where they grow agricultural products, such as vegetables, fruits and flour, strengthening family farming.

The fair operates from Monday to Saturday, with greater customer traffic on Fridays and Saturdays. Although each vendor's weekly profit is not high, any impediment to them selling will have a significant impact on their lives, depriving them of essential resources for their subsistence. Furthermore, floods, such as those that affect part of the fair during heavy rain, interrupt sales, causing losses to the city.

Considering current data on the number of stallholders and their average weekly profit, the estimated damage related to the fair's downtime (DDP) due to flooding could reach a total of R$ 250,000.00 in loss in 30 days, as shown the graph in figure 23.

Figure 23. Damage related to the days of shutdown in the affected areas.

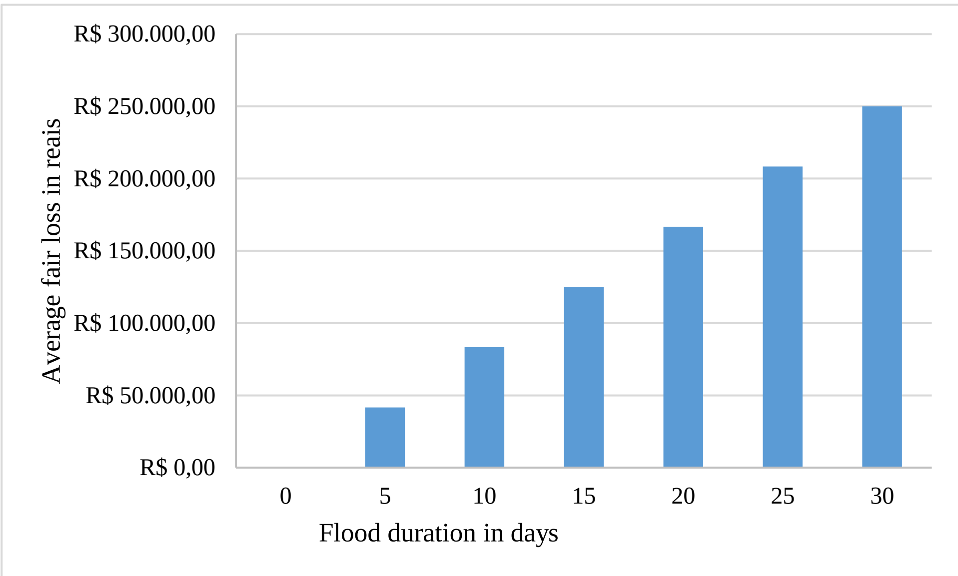

.

When analyzing the city's GDP per capita, characterized by R$ 11,003.76 (IBGE, 2022), it is clear that stallholders are part of the economically active population, representing 16.9% of the employed population.

With data from the flood analysis, linear regressions were performed to obtain mathematical equations that can be used to estimate the impact, in flooded area and water height, at different return times. The coefficients of determination R^2, which, the closer to 1, the better it demonstrates the adjustment of the model, were 0.85 and 0.98 for the variables flooded area and water height, respectively (Figures 24 and 25).

Figure 24. Linear regression for the estimated flooded area variable in return times.

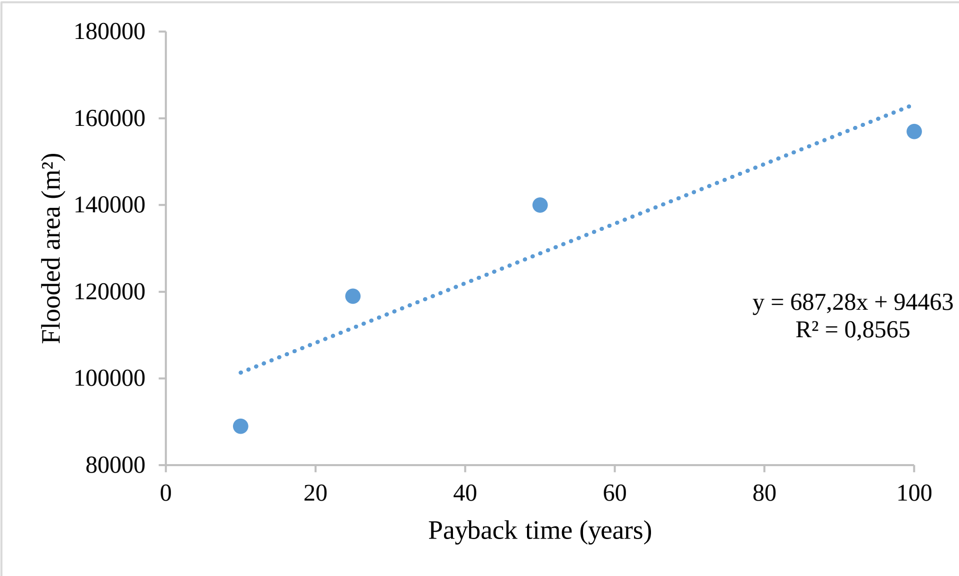

Figure 25. Linear regression for the variable water height estimated in return times.

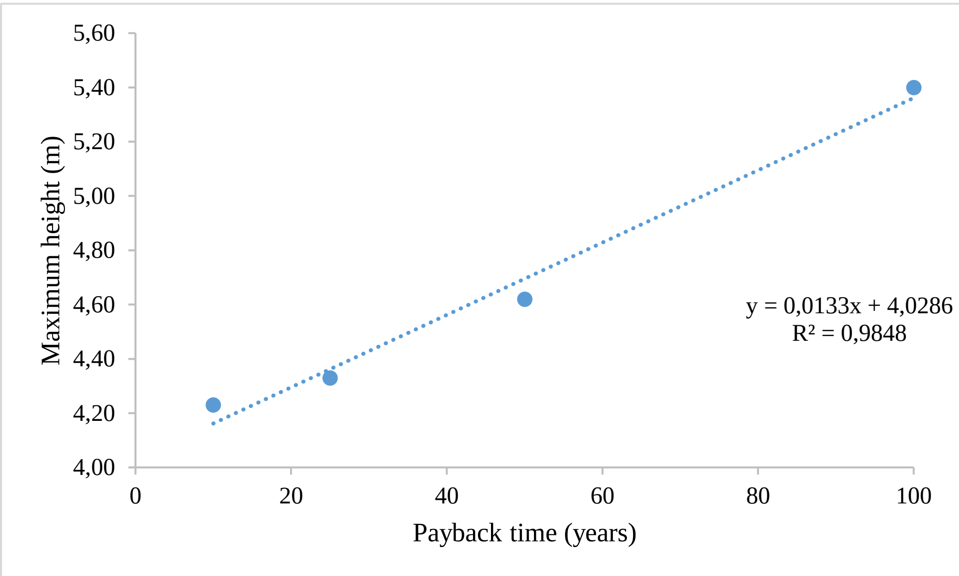

Considering data from flood analysis for return times of 10, 25, 50 and 100 years, floods at the fair were classified into 4 different levels and hypothetically determined the number of flood days stoppage for calculating financial losses due to DDP, presented in table 4:

Table 4. Hypothetical classification of floods at the fair based on return times and days of stoppage.

Return time	flood level	Downtime days
10 years	Small	4
25 years	Average	7
50 years	Big	10
100 years	Total	20

With the data in table 4 and figure 23, a linear regression was performed to obtain the mathematical equation that can be used to estimate the financial loss in reais at different payback times. The coefficient of determination R^2 was 0.99 (figure 26).

Figure 26. Estimation of financial loss at different payback times.

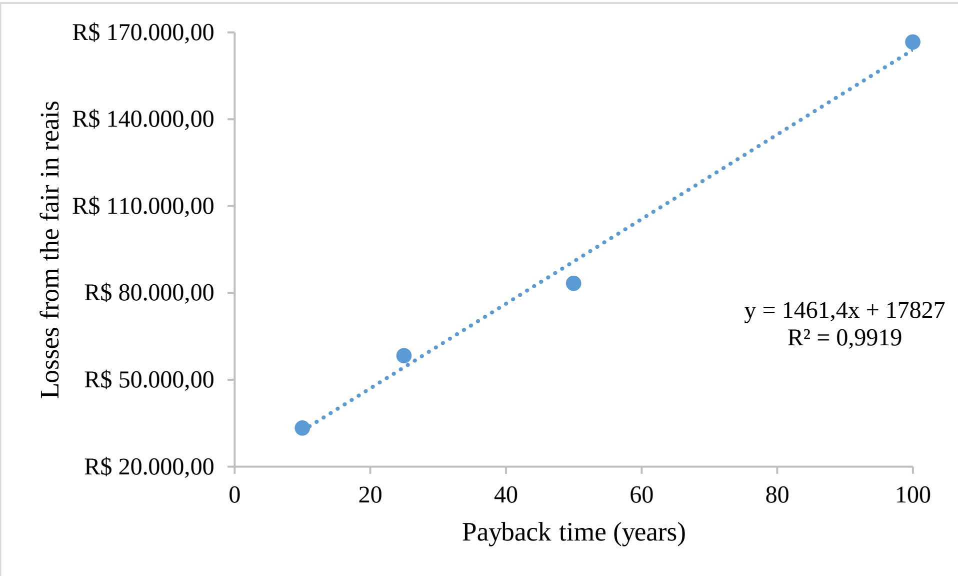

Considering a hypothetical situation based on the data obtained, for a flood with a return time of 75 years, the fair would be flooded in an area of 146,000 m², with a maximum water height of 5.03 m and a loss of around R$637 .00 per stallholder and R$ 127,432.00 total.

Furthermore, in the event of total flooding of the supply center, the city would have significant costs to rebuild the affected area. This highlights the relevance of this research for the local population.

The analysis of damage caused by floods was also based on studies, such as that of Fadel (2015) and Silva (2021), which quantified the economic losses associated with each flood level, as well as calculating the return times for each flood magnitude and the economic loss associated with it.

Based on this modeling presented, it is important to highlight that the damages used in this work do not cover all potential damages observed in a flood event, and may vary substantially depending on the characteristics of the region studied.

In summary, this research made it possible to measure the data caused to stallholders in relation to the days stopped in Catu – BA and also provided an assessment of the risks and losses associated with flood events, which are crucial for the formulation of risk management strategies and measures preventive. Furthermore, these results can serve as a basis for public policies aimed at strengthening local community resilience in the face of extreme weather events.

5 CONCLUSIONS

This study revealed important *insights* into flooding caused by rain in the Santa Rita neighborhood, in the city of Catu (Bahia). The neighborhood's proximity to the Catu River and the presence of a small dam were identified as factors that mitigate the impacts of flooding, since this area receives the flow of the three sub-basins.

The hydrological and hydrodynamic models, together with the QGIS software, played a fundamental role in building the simulation and analyzing the results. It is worth mentioning that this simulation took into account a moment in time; in the future, with increased waterproofing, the situation could worsen. Therefore, this research demonstrated the relevance of these simulations for the municipality, providing new insights into the behavior of flow and flooding in the area.

It is important to highlight that floods represent a danger to local commerce, street markets and human traffic, especially considering the 100-year return period. These areas become especially vulnerable in these extreme conditions.

Implementing solutions and strategies to manage heavy rainfall events is crucial to reducing economic losses and strengthening community resilience. According to the research problem initially identified, it was clear that floods cause serious damage to the market population of Catu, impacting both loss of life and economic losses.

We believe that by understanding the costs and economic damages associated with flooding, we could develop strategies and adaptation measures that would contribute to a more resilient and sustainable coexistence in the face of intense rainfall events.

These conclusions highlight the need for mitigation measures and adequate urban planning, aiming to minimize the risks and impacts of flooding. Understanding flood patterns, identifying high-risk areas, and developing stormwater management strategies are critical to promoting local community safety and resilience.

REFERENCES

ABREU, FG DE; NIECE, LA; BRANDÃO, JLB Analysis of the temporal distribution of rainfall in extreme hydrological events. **Sanitary and Environmental Engineering** , v. 22, no. 2, p. 239–250, 19 Jan. 2017.

ALMEIDA, L.; SERRA, J. C. V. Hydrological Models, types of most used applications. **Fae Magazine**, Curitiba, v. 20. n.1, p. 139 – 137, Jan /Jun. 2017.

ALVES, G. J. **Applicability of the CN-SCS method to a representative hydrographic basin of oxisols in the south of MG.** Federal University of Lavras (Master's dissertation), 2016.

ANA. National Water Agency. **HEC-RAS Basic Manual 5.0.3 Dam Break.** 2018.

ARAUJO, A. M.; RIBEIRO, E. M. Fairs and development: impacts of street markets on urban commerce in Jequitinhonha. **Brazilian Journal of Planning and Development** , v. 7, no. 2, p. 300, 29, 2018.

ARAÚJO, S. S. **Disaster Administration**: concepts and technologies. Emergency Planning Manual – State Secretariat for Civil Defense. Rio de Janeiro, 2012.

ASSIS, T. R. P *et al.* Impacts of rural producers' fairs on urban commerce in municipalities in the Jequitinhonha valley. **Proceedings of the XLIV Congress of the Brazilian Society of Rural Economics and Sociology.** Fortaleza, 2006.

BACK, Á. J.; OLIVEIRA, J. L. R.; HENN, A. Relationships between intense precipitation of different durations for the breakdown of daily rainfall in Santa Catarina. **Brazilian Journal of Agricultural and Environmental Engineering** , v. 16, no. 4, p. 391–398, apr. 2012.

BARBOSA, A. E.; FERNANDES, J. N.; DAVID, L. M. Key issues for sustainable urban stormwater management. **Water Research** , vol. 46, no. 20, p. 6787–6798 , Dec. 2012.

BENINI, S. M. **River dynamics in urban space: relevant aspects. National Magazine of City Management** . 2017

BIANCHI, C. I.; CAMPOS, P. M. B. G. M. A review of the study of environmental modeling tools to understand the real impact of cosmetic products on environmental safety. **Biomedical and Biopharmaceutical Research ,** vol. 20, no. 1, p. 126–135, 2023.

BORGES, P. G. **Hydrochemical study of groundwater in the Municipality of Catu-Bahia.** Federal University of Bahia, UFBA. 2015.

BRAZIL. Ministry of National Integration. National Secretariat of Civil Defense. Risk and Disaster Management Center. **Brazilian yearbook of natural disasters** , 2012. Available at: <http://www.mi.gov.br/c/document_library/get_file?uuid=e3cab906-c3fb-49fa-945d-649626acf790&groupId=185960> Accessed on : 13 Oct. 2023.

BRITO, P. L.; OLIVEIRA, G. A Characterization of Voluntary Geographic Information Applications in Hydrological Risk Management. **Brazilian Cartography Magazine**, Salvador p. 143-161, 2016.

CEPRANI, E.; MEDEIROS, J. S.; PALMEIRA, A, F. **Rainfall intensity**: a way of processing rainfall data to analyze the vulnerability of landscapes to soil loss. INPE, 2004.

CETESB - Environmental Sanitation Technology Company. **Urban drainage – Design manual** . 3rd ed. São Paulo: CETESB, 1986. 464p.

CHRISTOFOLETTI, A. **Modeling of Environmental Systems** . Edgart Publishing Blucher , 1st Edition, 2015.

DAMÉ, R. C. F.; TEIXEIRA, C. F. A.; TERRA, V. S. S. Comparison of different methodologies for estimating intensity-duration-frequency curves for Pelotas-RS. **Agricultural Engineering Magazine** , v.28, p.245-255, 2008.

DIGININO, R. S.; CARPI JUNIOR, S. Environmental Risk: concepts and applications. **Journal of Climatology and Landscape Studies** , Rio Claro, vol.2, p. 50, Jul /Dec. 2007.

DINIZ, M. T. M. Contributions to teaching the hypothetical-deductive method to Geography students. Geography. **Teaching & Research** , 19 (2), 107–111, 2015.

EMBRAPA. **Ecological Aspects – forests** . Available at: http://www.cnpf.embrapa.br/pesquisa/efb/aspec.htm. Accessed on: 12 Oct. 2023

FADEL, A.W. **Incorporation of loss risk in the management of flood control measures**. Masters dissertation. Federal University of Rio Grande do Sul, 2015.

FARIAS JUNIOR, J. E. F.; BOTELHO, R. G. M. **Comparative analysis of concentration time: a case study in the Cônego river basin, municipality of Nova Friburgo/RJ.** XIX Brazilian Symposium on Water Resources, 2011.

FERREIRA, J. C.; DANIEL, L. A.; TOMAZELA, M. Parameters for monthly equations for estimating maximum intensity precipitation for the State of São Paulo - Phase I. **Revista Ciência e Agrotecnologia** , v.29, p.1175-1187, 2005.

FESTA, GI *et al.* Calculating Economic Flood Damage through Microscale Risk Maps and Data Generalization: A Pilot Study in Southern Italy **. Sustainability** , 2022.

FIGUEIRAS, C. A. Environmental Modeling with uncertainty treatment in geographic information systems: The Geostatic flood paradigm. **National Institute for Space Research** . 2001.

FREITAS, C. M.; XIMENES, E. F. Floods and public health an issue in the recent scientific literature of causes, consequences and responses to prevention and mitigation. **Ciência & Saúde Coletiva** , 17(6):1601-1615, 2012.

GARCIA, F. R. **Comparison of MTDs based on the coupling of hydrological and hydrodynamic models applied to the identification of urban flooding areas.** Federal University of Bahia, UFBA. 2021.

GUIMARÃES, P. de O.; SANTOS, A. M. dos. Spatial analysis of deforestation factors in the Atlantic Forest Biome / Brazil. **GEOgraphies Magazine** , p. 1–19, 2023.

HORA, S. B. Mapping and risk assessment of flooding of the waterfall river in a section of the urban area of the municipality of Itabuna/BA. **Society & Nature** , Uberlândia, 21 (2): 57-75, Aug. 2009.

IBGE. Brazilian Institute of Geography and Statistics. **Catu.** 2023. Available at < https://cidades.ibge.gov.br/brasil/ ba / catu / historico > Accessed on: 13 Oct. 2023.

IBGE. Brazilian Institute of Geography and Statistics. **Catu:** Population. 2022. Available at <https://cidades.ibge.gov.br/brasil/ba/catu/ > Accessed on: 13 Oct. 2023.

INMET. **Climatological normals in Brazil** . Available at <https://portal.inmet.gov.br/normal> Accessed on: 18 Nov. 2023.

JONOV, C. M. P; NASCIMENTO, N. O. F. O.; SILVA, A. de P. E. Assessment of damage to buildings caused by floods and obtaining recovery costs. **Built Environment,** v. 13, no. 1, p. 75–94, mar. 2013.

KUREK, R. K. M. **Assessment of the Return Time of Flood Levels in Vale do Taquari/RS**. Univates University Center . 2012.

LEITÃO, F. T. **1d, 1d/2d and 2d hydrodynamic modeling of the tidal effect in the Cocó River** (Master's dissertation). Fortaleza, 2018.

LOURENÇO, G. M. **Economic Indicators.** University of Rio Grande do Sul, UFRGS. 2002

LOURENÇO, L.; NUNES, A. Hydrometeorological Risks . **Portuguese Association of Risks** , **Prevention and Security** , Coimbra. 2018.

MAPBIOMES. **MapBiomas Collections** . Available at: https://mapbiomas.org/colecoes-mapbiomas1?cama_set_language=pt-BR. Accessed on: 13 Oct. 2023.

MARINHO FILHO, G. M. M. *et al.* Hydrological models: concepts and applicability. **Environmental Sciences Magazine** , Canoas; v.6, p35 to 47. 2012.

MARTEL, J. L. *et al.* Climate Change and Rainfall Intensity–Duration–Frequency Curves: Overview of Science and Guidelines for Adaptation. **Journal of Hydrologic Engineering** , vol. 26, no. 10, Oct. 2021.

BRUNO, L. S.; MATOS, T. S.; OLIVEIRA, P. T. S. Hydrographic Basin Modeling with HEC – RAS. **Federal University of Minas Gerais** , 2021.

MELLO, C. R. *et. al.* Kriging and inverse square of the distance for interpolation of the parameters of the heavy rainfall equation. **Brazilian Journal of Soil Science** , v.27, p.925-933, 2003

MENEZES, M. A. A. **Professional education, family farming and local and regional development: the federal institute of education in Bahia catu *campus* .** Salvador University , UNIFACS. 2011.

MOUNT, B. E. O.; GOLDENFUM, J. A.; MICHEL, G. P.; CAVALCANTI, J. R. de A. Terminology of natural hazards and disasters: A review and the case of Brazil. **International Journal of Disaster Risk Reduction** , vol. 52, p. 101970, Jan. 2021.

MOREIRA, P. G. *et al.* Estimation of the parameters of intense rainfall intensity-duration-frequency equations for the state of Bahia, Brazil. **REDE - PRODEMA Electronic Magazine** , Fortaleza, v. 1, no. 14, p. 151-164, Feb. 2021. 2020.

NYAMATHI, S. J.; KUMAR, H. K. Y. Generation of Intensity Duration Frequency Curve Using Daily Rainfall Data for Aghanashini River Watershed. **Uttara Kannada** , 2021. p. 647–654.

OKADA, O. K. **River Runoff and Hydrological Risks in Mountain Basins of the Montesinho Natural Park , NE Portugal: spatial variability and temporal trends.** Federal Technological University of Paraná. 2019.

OLIVEIRA, A. M. de. **Mapping of areas susceptible to flooding due to dam failure in a semi-arid environment.** University of São Paulo (PhD thesis in Physical Geography). P. 1-142. 2016.

OLIVEIRA, E. L. A. Vulnerability: The Central Question of the Risk Equation. **Geography, Teaching and Research** , vol. 22, p. 01-09, 2018.

OLIVEIRA, L. F. C.; ANTONINI, J. C.; GRIEBELER, N. Methods for estimating maximum precipitation for the State of Goiás. **Brazilian Journal of Agricultural and Environmental Engineering** , v. 12, p. 620-625, 2008.

ORTIZ, J. A. V.; MARTÍNEZ-GRAÑA, AM Calculation of precipitation and seismicity thresholds as triggers for mass movements in the region of Bucaramanga, Colombia. **Ecological Indicators**, vol. 152, p. 110355, Aug. 2023.

PEREIRA, J. M. A *et al.* Impact of climate change on public health: integrative review. Electronic *Magazine* **Acervo Saúde**, v. 12, no. 11, p. e4720, nov. 2020.

PEREIRA, S. B. *et al*. Precipitation Intensity, Duration and Frequency Equation for the Dourados Region, MS. **Brazilian Agricultural Research Corporation (Embrapa),** 2007.

PORCIÚNCULA, R. DE J.; LIMA, O. A. L. de; LEAL, L. R. B. Geoelectric method - potential instrument to help manage soil and underground water resources: case studies, Alagoinhas, Bahia. **XIX Brazilian Groundwater Congress**. 2016.

PRINA, B. Z.; TRENTIN, R. Flood return time: methodological application. **Geousp – Space and Time** (Online), v. 22, no. 3, p. 670-686, Dec. 2018. ISSN 2179-0892

REIS, P. A.; SCHMIDT, M. A. Evaluation of the HEC-RAS and GRASS Models in identifying Areas Vulnerable to Flooding in Urban Areas. **Yearbook of the Institute of Geosciences – UFRJ** . v. 1, 115-126, 2017.

RENNÓ, C. D.; SOARES, J. V. **Chapter 2: Basic Concepts of Hydrological Modeling.** 2002

RODRIGUES, R. S. S. *et al.* Analysis of the effects of an extreme rainfall event on surface runoff in a small rural Amazonian river basin. **Brazilian Journal of Climatology** , v. 26, no. April 2018, p. 368–392, 2020.

SANTOS, S. R. Q. *et al.* Frequency of extreme drought and rain events in Amazon using different precipitation data bases. **Brazilian Journal of Physical Geography** , v. 10, no. 2, 2017.

KNOW. Superintendency of Economic and Social Studies of Bahia. **Analysis of Climate Attributes of the State of Bahia** . 1999.

SILVA NETO, V. L. *et al.* Intensity-duration-frequency relationship (IDF) for extreme precipitation in Guaraí-TO . **Biosphere Encyclopedia** , v. 13, no. 23, p. 1147, 2016.

SILVA, D. F. *et al.* Characterization of extreme events and their climatic causes based on the Standardized Precipitation Index for the East of the Northeast. **Brazilian Journal of Physical Geography** , v. 13, no. 2, p. 449–464, 7 Apr. 2020.

SILVA, E. D. Determination of the severe flood quota based on the criterion of associated economic losses: application to the municipality of São Sebastião do Caí - RS. **XXIV Brazilian Symposium on Water Resources,** 2021.

SIQUEIRA, R. C. **Proposal of a methodology for constructing a flood risk graph in urban basins: case study of the Cachoeirinha stream basin.** UFMG School of Engineering . 2017.

SOBIERAJ, J.; BRYX, M.; METELSKI, D. Stormwater Management in the City of Warsaw: A Review and Evaluation of Technical Solutions and Strategies to Improve the Capacity of the Combined Sewer System. **Water** , vol. 14, no. 13, p. 2109, 1 July. 2022.

SOPRANI, M. A.; REIS, J. A. T. Proposition of precipitation Intensity-Duration-Frequency equations for the Benevente river basin, ES. **Revista Capixaba de Ciência e Tecnologia** , v.1, p.18-25, 2007.

TACHINI, M. **Assessment of damages associated with floods in the municipality of Blumenau** . Thesis (Postgraduate Program in Environmental Engineering) – Federal University of Santa Catarina, 2010.

TEMEZ, JR Hydrometeorological calculation of maximum flows in small cuencas naturales . Madrid: Ministry of Public Works and Urbanism (MOPU). **General Directorate of Carreteras** , n. 12, 1978.

TEODORO, P. H. M.; NUNES, J. O. R Flooding in Presidente Prudente SP: a interdisciplinary work based on geological mapping. **Revista Formação**, n.17, volume 2 – p. 81-102. São Paulo, 2007.

TUCCI, C. E. M. (Org.). **Hydrology**: science and application. São Paulo/Porto Alegre: Edusp/UFRGS, chap. 16. p. 621-658, 1993.

TUCCI, C. E. M. Urban Drainage Master Plan: Principles and Design. **Brazilian Journal of Water Resources** , vol.2 – Jul /Dec, 2007

US ARMY CORPS OF ENGINEERS (USACE). **HEC-RAS: river analysis system, user's manual** . Davis: Hydrologic Engineering Center, 2002.

USACE-HEC. **Hydrologic Modeling System, HEC-HMS v3.3 – User's Manual** , US Army Corps of Engineers, Hydrologic Engineering Center, September 2008.

WEATHERSPARK. **Climate and average weather conditions in Catu all year round** . 2023. Available at <https://pt.weatherspark.com/y/31064/Clima-caracter%C3%ADstico-em-Catu-Brasil-durante-o-ano#:~:text=Chove%20ao%20longo% 20 of%20year,thousand%C3%ADmeters%20of%20precipitates%C3%A7%C3%A3o%20of%20rain.> Access on : 13 Oct. 2023.

WESTRA, S. *et al.* Future changes to the intensity and frequency of short-duration extreme rainfall. **Reviews of Geophysics** , vol. 52, no. 3, p. 522–555, Sept. 2014.

WINKLER, A. S. *et al.* Estimation of the concentration time of a river basin: comparison between methodologies. **XVIII CIC - XI EPOS I Scientific exhibition** , 2009.

ATTACHMENT

Annex 1. Hyetogram Table for return times of 10, 25, 50 and 100 years

Instante (min)	Intensidade (mm/h)	Precipitação acumulada (mm)	Precipitação (mm)	Precipitação Alternada (mm)
5	129.87	10.82	10.82	1.49
10	107.23	17.87	7.05	1.82
15	91.97	22.99	5.12	2.33
20	80.91	26.97	3.98	3.23
25	72.49	30.20	3.23	5.12
30	65.84	32.92	2.71	10.82
35	60.43	35.25	2.33	7.05
40	55.95	37.30	2.05	3.98
45	52.16	39.12	1.82	2.71
50	48.91	40.76	1.64	2.05
55	46.09	42.25	1.49	1.64
60	43.61	43.61	1.37	1.37

Instante (min)	Intensidade (mm/h)	Precipitação acumulada (mm)	Precipitação (mm)	Precipitação Alternada (mm)
5	151.21	12.60	12.60	1.74
10	124.85	20.81	8.21	2.12
15	107.08	26.77	5.96	2.72
20	94.20	31.40	4.63	3.76
25	84.40	35.17	3.76	5.96
30	76.65	38.33	3.16	12.60
35	70.36	41.04	2.72	8.21
40	65.14	43.43	2.38	4.63
45	60.73	45.55	2.12	3.16
50	56.94	47.45	1.91	2.38
55	53.66	49.19	1.74	1.91
60	50.78	50.78	1.59	1.59

Instante (min)	Intensidade (mm/h)	Precipitação acumulada (mm)	Precipitação (mm)	Precipitação Alternada (mm)
5	169.65	14.14	14.14	1.95
10	140.07	23.35	9.21	2.38
15	120.14	30.03	6.69	3.05
20	105.69	35.23	5.20	4.22
25	94.69	39.45	4.22	6.69
30	86.00	43.00	3.55	14.14
35	78.94	46.05	3.05	9.21
40	73.08	48.72	2.67	5.20
45	68.13	51.10	2.38	3.55
50	63.89	53.24	2.14	2.67
55	60.20	55.19	1.95	2.14
60	56.97	56.97	1.79	1.79

Instante (min)	Intensidade (mm/h)	Precipitação acumulada (mm)	Precipitação (mm)	Precipitação Alternada (mm)
5	190.34	15.86	15.86	2.18
10	157.15	26.19	10.33	2.67
15	134.79	33.70	7.50	3.42
20	118.58	39.53	5.83	4.74
25	106.24	44.27	4.74	7.50
30	96.49	48.24	3.98	15.86
35	88.57	51.66	3.42	10.33
40	81.99	54.66	3.00	5.83
45	76.44	57.33	2.67	3.98
50	71.68	59.73	2.40	3.00
55	67.54	61.92	2.18	2.40
60	63.92	63.92	2.00	2.00

Source: Author (2023).